# DESIGN OF OPEN HYDROGEN-BONDED FRAMEWORKS USING BIS(IMIDAZOLIUM 2,4,6-PYRIDINETRICARBOXYLATE)METAL COMPLEXES AS SECONDARY BUILDING UNITS

By

Mehmet Veysel Yigit

A Thesis submitted to the Faculty of the

Department of Chemistry & Biochemistry

Worcester Polytechnic Institute

Worcester, MA 01609-2280, USA

In partial fulfillment of the requirements for the

Degree of Master of Science

In Chemistry

By

_____

*date*

Approved:

---

Dr. John C. MacDonald, Major Advisor

---

Dr. James P. Dittami, Department Head

**Abstract:** The supramolecular chemistry and crystal structures of four Bis(imidazolium 2,4,6-pyridinetricarboxylate) metal(II)dihydrate complexes, where M=$Co^{2+}$, $Ni^{2+}$, $Cu^{2+}$, or $Zn^{2+}$ (**1-4**, respectively), are reported. These complexes serve as supramolecular building blocks that self-assemble when crystallized to generate a single, well defined structure in the solid state. 2,4,6-Pyridinetricarboxylate anions and imidazolium cations form strong ionic hydrogen bonds that dominate crystal packing in compounds **1-4** by forming three-dimensional (3-D) networks of molecules. These networks consist of hydrogen-bonded layers of molecules defined by N-H···O interactions that are joined in the third dimension by O-H···O interactions. This 3-D network provides a supramolecular framework with which to control and predict molecular packing by design for engineering the structures of crystals. Furthermore, compounds **1-4** create a robust organic host lattice that accommodates a range of different transition metals without significantly altering the molecular packing. Growth of crystals from solutions that contain two or more different metal complexes results in the formation of mixed crystals in which the different metal complexes are incorporated into the crystalline lattice in the same relative molar ratio present in solution. Epitaxial growth of crystals involving deposition of one metal complex on the surface of a seed crystal that contains a second metal complex generates composite crystals in which the different metal complexes are segregated into different regions of the crystals. Compounds **1-4** form crystalline solids that represent a new class of modular materials in which the organic ligands serve as a structural component that defines a single packing arrangement that persists over a range of structures, and in which the metal serves as an interchangeable component with which vary the physical properties of material.

**Acknowledgements**

I would like to thank my advisor Prof. John C. MacDonald for his outstanding support and patience during this research. I appreciated the opportunity to work with him. The scientific fundamentals that I learned from him are going to build my future academic career.

I also would like to thank my friends and colleagues Brian Moulton, Christopher Cooper, Dr. Hubert Nienaber.

Finally I thank all chemistry and biochemistry faculty and graduate students for making this an enjoyable time.

**TABLE OF CONTENTS:**

**LIST OF FIGURES:**

**LIST OF TABLES:**

## Introduction

The field of crystal engineering has undergone tremendous growth over the past ten years.[1-4] Recently, a number of reports on crystalline organic and metal-organic materials that exhibit micro- and nanoporous behavior have been reported with crystalline structures that are stable upon removal of guest molecules.[5-9] Such porous materials have potential for commercial application in areas such as molecular separations, catalysis, storage, photonic materials and synthetic zeolytes.[10,11] Consequently, there is a growing interest to develop strategies and methodologies to construct new types of porous materials with properties that can be designed, predicted and manipulated. Current efforts in this area are aimed at controlling parameters such as the size and shape of channels and cavities, surface exposed functional groups, trapping or exchange of guest molecules, molecular recognition and selectivity.[12,13] General methodologies to design, synthesize and utilize porous crystalline materials have not been realized yet despite significant progress toward understanding molecular self-assembly in solids, and the development of many interesting new materials.

In order for porous crystalline materials to be useful, it is important that their crystal structures and molecular packing can be predictably tuned by altering the functional groups and structures of the molecular building blocks from which they are constructed.[14,15] Efforts to develop new

molecular components for this purpose have focused primarily on the design of building blocks composed of organic molecules and coordination compounds. Recent literature in this area shows that several principles have emerged regarding the rational design of porous materials: (1) an ideal porous solid is one in which the molecular building blocks self-assemble under thermodynamic conditions in solution to create a three-dimensional framework; (2) the framework should form large channels or cavities with long-range order that permeate the lattice and enclose molecules of solvent; (3) the void volume of the channels or cavities should be large relative to the size of enclosed molecules of solvent to ensure that the solvent can be removed under vacuum or by heating, or exchanged with other guests. Accordingly, there are a number of challenges that must be considered for rational and designed synthesis of porous materials to become reality. Four of these challenges are described in the following paragraphs.[16]

First, it can be difficult to control the assembly of molecular building blocks during the process of crystallization in order to achieve a given three-dimensional architecture, or molecular framework. Molecular building blocks with multiple sites for hydrogen bonding or metal-ligand coordination frequently form multiple frameworks that have different structures or intermolecular connectivity.[16]

Second, supramolecular aggregates composed of many molecules generally are less soluble than the individual molecules. This lower solubility can lead to kinetically driven processes of molecular aggregation that inhibit crystallization and result in the formation of poorly crystalline or amorphous solids that are difficult to characterize using X-ray diffraction.[16]

Third, it is difficult to promote the formation of robust crystalline solids with large channels or cavities that remain open. Maximization of favorable enthalpic interactions between molecules during crystallization often leads to interpenetration in which two or more separate frameworks intertwine within the same crystalline lattice. Interpenetration of one framework within another poses serious problems in the design of porous materials since it leads to a reduction in the void volume available for guests within channels or cavities. Unfortunately, interpenetration is pervasive in crystalline solids that feature two- and three-dimensional frameworks.[16] Trimesic acid (1,3,5-benzenetricarboxylic acid) provides an extreme example of this phenomenon in which each two-dimensional honeycomb framework is interpenetrated by six other independent frameworks.[17,18] Although stacking of honeycomb frameworks has the potential to create channels with enormous void volumes (i.e., greater than 50% of the volume of the crystal), interpenetration renders crystals of trimesic acid nonporous.

Fourth, frameworks with pores that incorporate solvent frequently are too fragile to withstand removal of solvent molecules. Although many examples of crystalline frameworks are known that trap solvent and other guest molecules present in solution during growth of crystals, the majority of these frameworks decompose or undergo irreversible structural rearrangement to nonporous structures upon removal of solvent or guests.[16]

**Background**

Currently, the most prevalent strategy for engineering the structures of crystals takes advantage of directional intermolecular interactions between molecules as the principle means of controlling molecular assembly during crystallization.[14,15] For example, the literature contains numerous examples of organic crystals in which hydrogen bonds are used to generate supramolecular assemblies of organic molecules with structures that can be controlled selectively in one, two and three dimensions.[19-21] Examples of such structures are shown in Figures 1, 2, and 3, respectively, for molecular building blocks that contain amide functional groups. In these structures, the amide N-H and C=O groups drive assembly of the molecular building blocks by forming intermolecular N-H···O hydrogen bonds between neighboring molecules. Leiserowitz has demonstrated

conclusively that primary and secondary amides self-associate as a general rule by forming hydrogen-bonding interactions of this sort.[22,23]

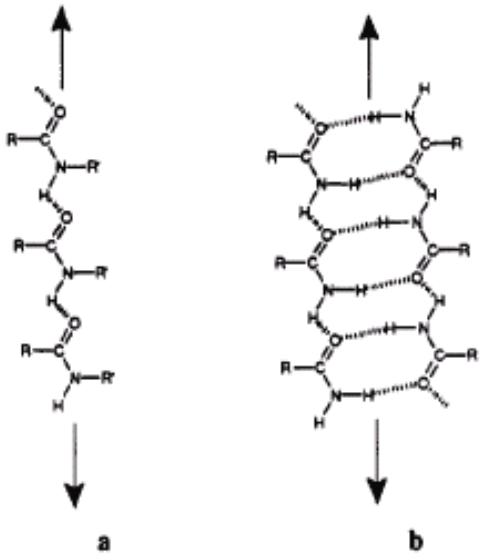


**Figure 1**: Examples of one-dimensional growth. The drawing on the left **(a)** shows one-dimensional assembly of a secondary amide. The drawing on the right **(b)** shows one-dimensional assembly of a primary amide.

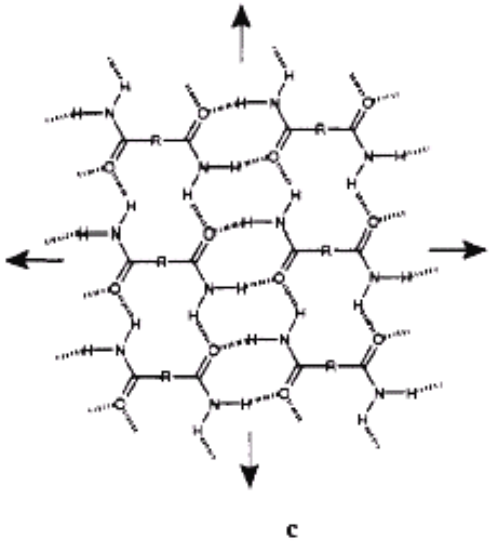


**Figure 2:** Common hydrogen-bonding pattern for primary diamides. An example of two-dimensional self-assembly.

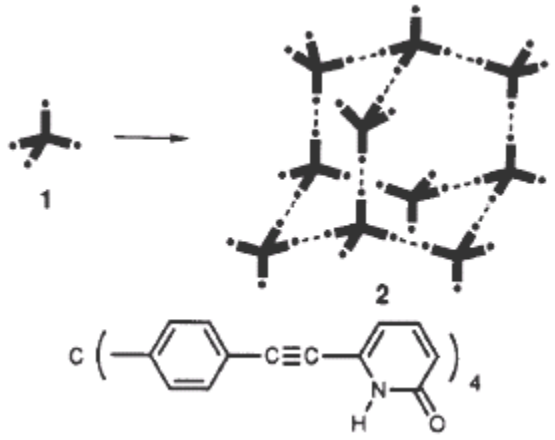


**Figure 3:** Self assembly of tetrapyridone results in a three-dimensional organic diamondoid network. [24]

Crystalline materials composed of organic compounds are attractive from the standpoint of crystal engineering because organic molecules exhibit a wide range of physical properties that are modified easily through synthesis. Although many interesting structures have been discovered, the goal of achieving functional materials from organic crystals, and porous crystalline materials in particular, has not been realized, especially when compared to materials based on organic polymers and inorganic compounds. One potential drawback of purely organic crystal is their relatively low thermal and mechanical stability, which can render them ineffective as materials for devices.[25] Another problem is the tendency of organic compounds with several different functional groups to form more than one pattern of hydrogen bonds. This situation can promote the formation of polymorphs that have different physical properties.[21,26-29] Polymorphs are different crystalline forms, or solid phases, of the same compound that arise when the molecules crystallize with different packing arrangements. For example, flat coin-shaped molecules might pack by forming parallel stacks of molecules in one crystalline form and a herringbone arrangement in a second crystalline form. Polymorphs generally exhibit different physical properties such as crystal morphology (shape), melting point, hardness, color, and porosity, among others. An example of two polymorphs (forms I and II) of the organic compound nabumetone and the corresponding crystal packing arrangements are shown in Figure 4.[30] Polymorphism is problematic from the standpoint of

crystal engineering and the design of materials with predictable structures because the lattice energies of polymorphs typically differ only by about 0.5 kcal/mol. At present, the occurance of polymorphs cannot be predicted reliably using computational methods.

**Form I** **Form II**

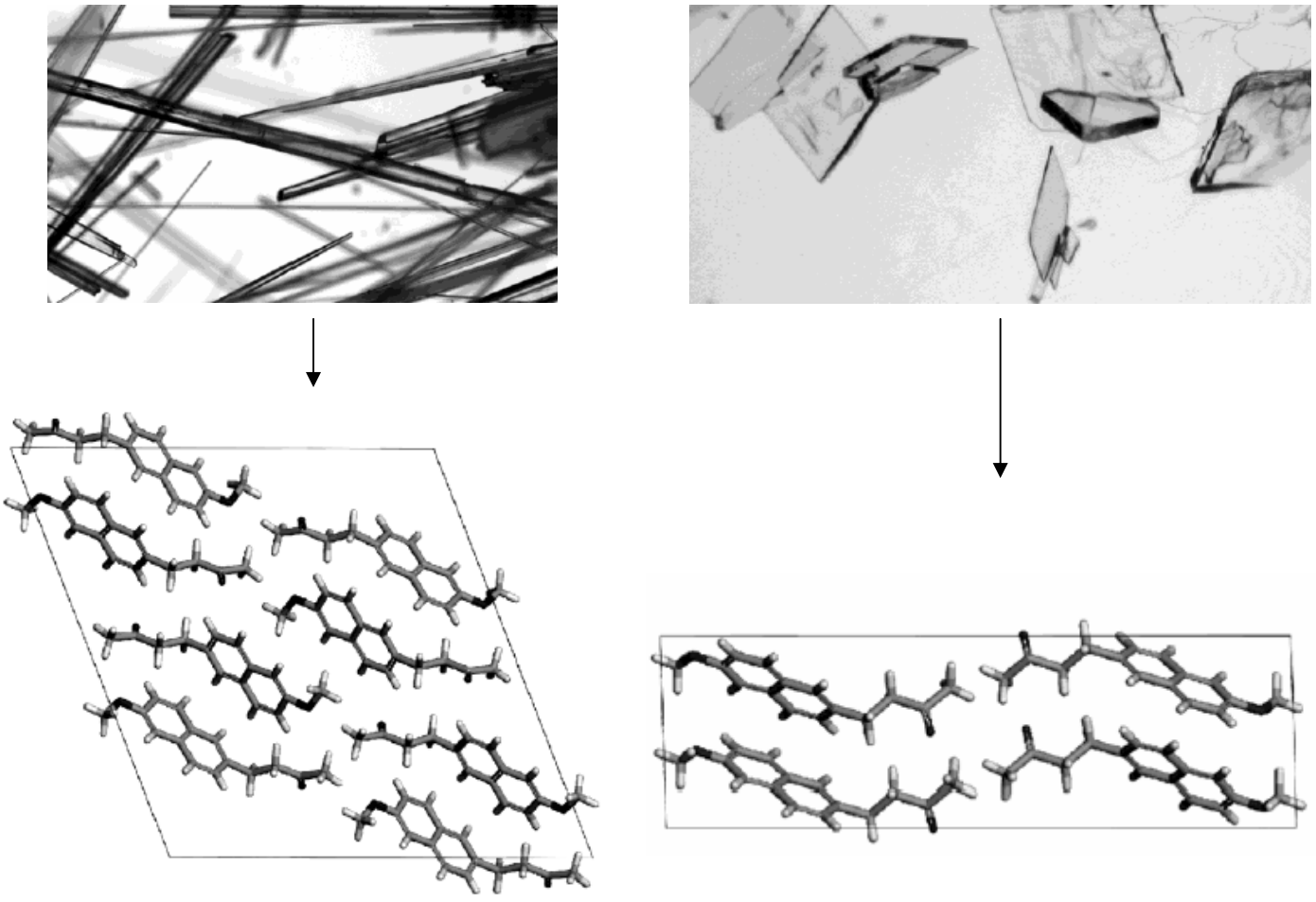

**Figure 4:** Two polymorphs of nabumetone. Form I on the left , Form II on the right. Packing diagrams of polmorphs are illustrated below the crystals.

An alternative approach to crystal engineering uses metal-ligand bonds between transition metals and organic ligands to create coordination polymers that have extended structures.[2,12,31-39] Coordination compounds have advantages over organic compounds as molecular building blocks because metals exhibit a variety of coordination geometries and a broad range of physical properties that are understood. A potential disadvantage of coordination polymers is that the strength of metal-ligand bonds is typically at least an order of magnitude greater than that of hydrogen bonds. Consequently, supramolecular structures of some coordination polymers can be very rigid, form irreversibly, and exhibit such fast kinetics for nucleation and growth of crystals that the products form insoluble microcrystalline powders.[25] Yaghi recently has reported a new family of porous materials constructed using this type of strategy.[40] In these systems, organic dicarboxylic acids combine with transition metals to form more complex octahedral building units. These building units assemble further into open metal-organic frameworks with porous channels that account for 91% of the crystal volume. These remarkably porous materials trap molecules of solvent that can be removed under vacuum and then used to store gases such as methane. Examples of several metal-organic frameworks that have been successfully built by his group are shown in Figure 5.

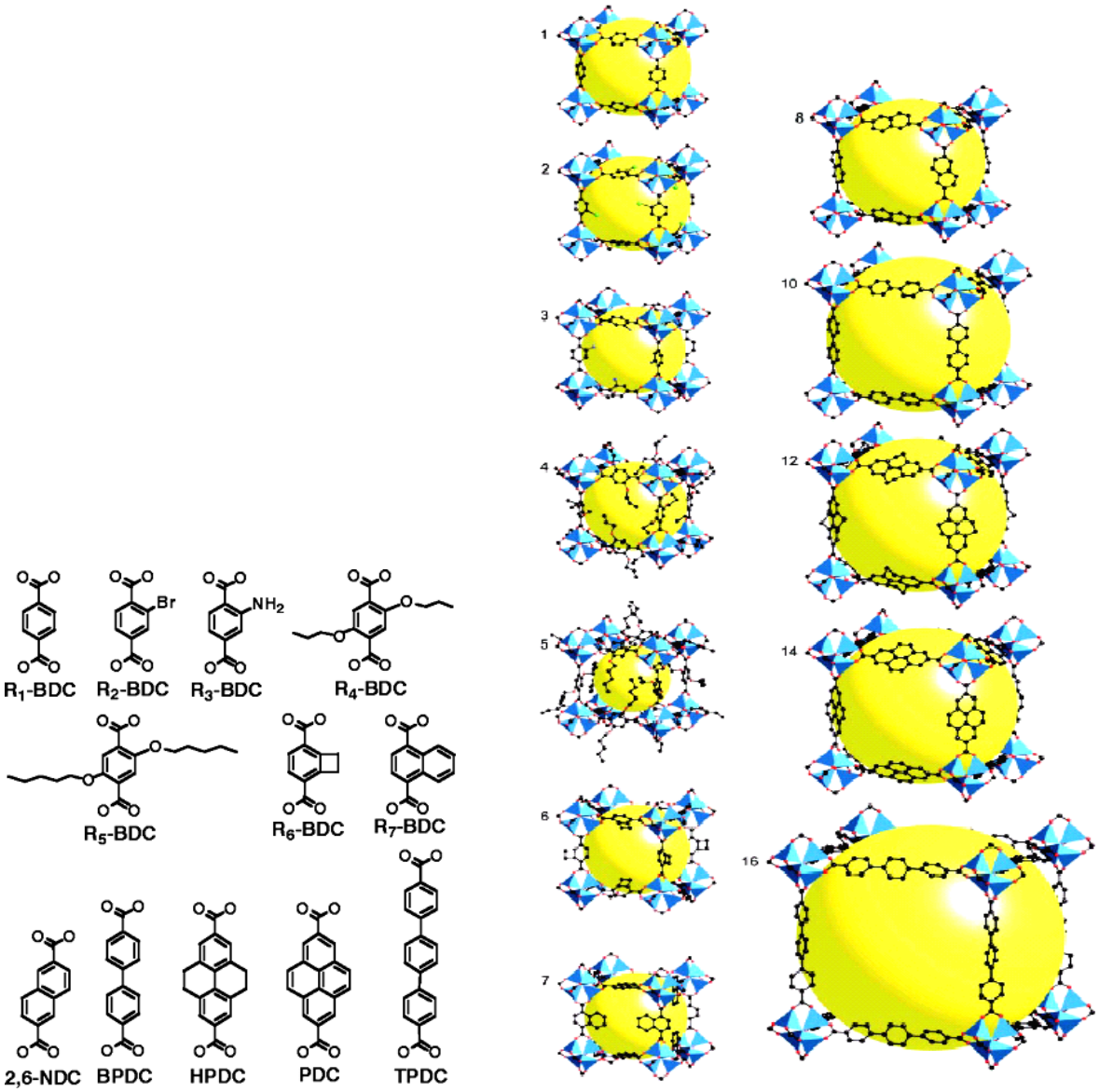


**Figure 5:** Metal-organic frameworks of various ligands having free volumes in crystals ranging from 55.8% to 91.1% of total crystal volume. Ligands are shown on the left.[40]

.

We have chosen deliberately to work with materials that contain both organic molecules and transition metals because coordination compounds offer a wide range of molecular structures that are accessible through relatively simple organic and inorganic synthesis. In addition, transition metals are attractive for the design of materials because they offer unusual optical and electronic properties that are not available in purely organic materials. [41-46]

Recent efforts in our group have focused on the design of layered crystalline materials as a first step toward controlling molecular assembly in three dimensions. This work involved using hydrogen bonds, or a combination of hydrogen bonds with metal-ligand bonds, as design elements to direct molecular assembly in two dimensions. We wanted to determine if this approach provides a means to control the rigidity of a supramolecular framework of molecules joined by metal-ligand interactions by selectively incorporating more flexible hydrogen bonds between molecules. We have found that constraining molecules to assemble into layers has several advantages from the standpoint of design and control over bulk crystalline structure: it significantly reduces the degrees of translational freedom available to individual molecules while packing; it limits molecular packing to just a few possible packing arrangements by defining the relative position and orientation of molecules within layers, and it reduces the problem of predicting crystal

packing in three-dimensions from that of individual molecules to that of well-ordered layers of molecules.

To illustrate these advantages, we have shown that hydrogen bonding in organic salts between imidazolium cations and anions of dicarboxylic acids effectively locks the ions into layers. An example of one such layer from the crystal structure of imidazolium hydrogen fumarate is shown in Figure 6.[47]

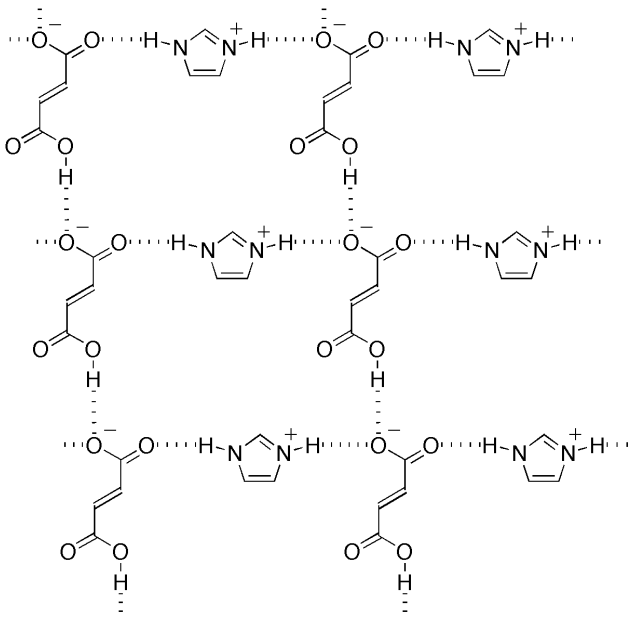

**Figure 6:** Hydrogen-bonded layer formed in the crystal structure of imidazolium hydrogen fumarate.[47]

The anions of dicarboxylic acids form hydrogen-bonded chains (O-H·····O) of anions that align in parallel rows. This pattern is prevalent in salts of tartaric and malic acids as well.[48-50] These chains are cross-linked into layers by imidazolium cations that form a second set of hydrogen-bonded chains ($^{+}$N-H·····O$^{-}$). Layers of this type are ubiquitous in imidazolium carboxylate salts. Moreover, they contain ionic hydrogen bonds that are strong, yet flexible enough to accommodate a range of substituents without disrupting the layer motif. We have used hydrogen bonding between imidazolium cations and carboxylate anions as an element for design in the work described in this thesis.

We also have shown recently that imidazolium bis(2,6-pyridinedicarboxylate) metal(II) salts (M = Mn, Co, Ni, Cu, Zn) form an isostructural series in which the cations and anions form layers. A representative example of one such layer from the crystal structure of the imidazolium bis(2,6-pyridinedicarboxylate) copper(II) salt is shown in Figure 7. [25]

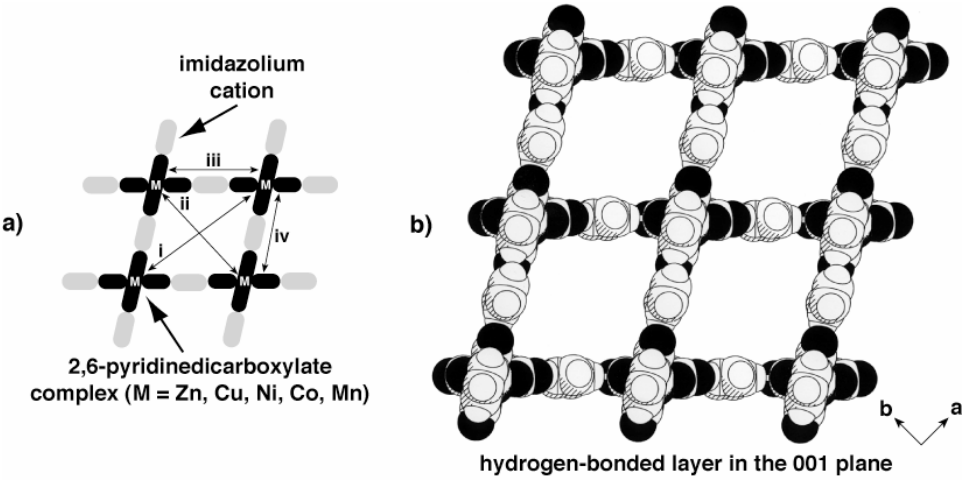


**Figure 7:** Layer framework formed in the crystal structure of imidazolium bis(2,6-pyridinedicarboxylate) copper(II). a) Schematic representation of crystal packing showing the distances between imidazolim cations (grey) and bis(2,6-pyridinedicarboxylate) anions (black): i = 21.5 Å, ii = 16.9 Å, iii = 13.7 Å, iv = 13.7 Å. b) A space-filling model shows the structure of a single layer. [25]

Individual layers form open two-dimensional frameworks that feature regular arrays of pores separated by 14 Å. In the crystals, these pores are no empty in the crystal but rather are filled by pyridyl rings that project outward from adjacent layers. We hypothesize that these layers have excellent potential to form large channels (i.e., ~ 10 Å across) if the pores can be aligned when then layers stack. This hypothesis provides much of the impetus for the current work described in the sections that follow.

**Current Work**

Our goal is to make porous solids with open channels. In order to achieve our goal we want to develop a strategy to extend control of molecular assembly from two dimensions to three dimensions. For that reason we want to design new molecular building blocks by incorporating additional hydrogen-bonding functionality on the 2,6-pyridinedicarboxylate ligand. We want to determine whether these new building blocks promote formation of layered frameworks with structures similar to those present in imidazolium bis(2,6-pyridinedicarboxylate) metal(II) complexes. We propose that additional hydrogen-bonding groups on the pyridyl ring will promote stacking of such 2-D frameworks and provide control in three dimensions over the spacing and alignment of pores between adjacent layers. We expect that crystalline materials grown using this strategy will include or trap molecules of solvent in channels that are aligned in parallel. We want to determine if these types of materials feature robust

host frameworks that exhibit porous behavior where guest molecules can be removed under vacuum or by heating and exchanged without the host losing structural integrity. We also want to determine if complexes with the same organic ligands but different transition metals form an isostructural series both in terms of molecular structure of the metal complex and crystal packing. Metal complexes that form an isostructural series are of interest because they present a class of molecular building blocks in which the metal component can be exchanged with different metals without altering the resulting molecular structure and crystal packing. We want to investigate whether different metal complexes with metals such as Co, Ni, Cu and Zn can be used in combination to form mixed and composite crystals. We have show previously that imidazolium bis(2,6-pyridinedicarboxylate) metal(II) complexes from an isostructural series where the complexes with Mn, Co, Ni, Cu and Zn can be mixed together to form mixed crystals that contain combinations of two or more metals in the same crystalline lattice. We also have shown previously a crystal of one imidazolium bis(2,6-pyridinedicarboxylate) metal(II) complexes can be used as a seed on which to initiate epitaxial growth of an outer layer of a second metal complex. These mixed and composite crystals represent new classes of crystalline materials whose optical and physical properties can be manipulated as a function of the types and relative ratios of metals that are present in the crystal. Moreover, mixed and composite crystals are modular materials in which the organic ligands

define a single persistent molecular structure and crystal packing, and in which the metal component can be exchanged. Accordingly, we want to investigate whether new metal complexes that provide control of molecular assembly in three dimensions via hydrogen bonding also will form mixed and composite crystals with physical properties similar to those of imidazolium bis(2,6-pyridinedicarboxylate) metal(II) complexes.

Based on the goals above, we chose to synthesize a new class of building blocks using 2,4,6-pyridinetricarboxylic acid (246PTA) as the organic ligand for several reasons. 246PTA has the same molecular structure as 2,6-pyridinedicarboxylic acid with an additional carboxyl group at the 4-position of the pyridyl ring. Therefore, we expected 246PTA to form tetrahedral complexes with $Co^{2+}$, $Ni^{2+}$, $Cu^{2+}$, $Zn^{2+}$ transition metal ions and that these complexes would have structures similar to those with 2,6-pyridinedicarboxylic acid as shown in Figure 8.

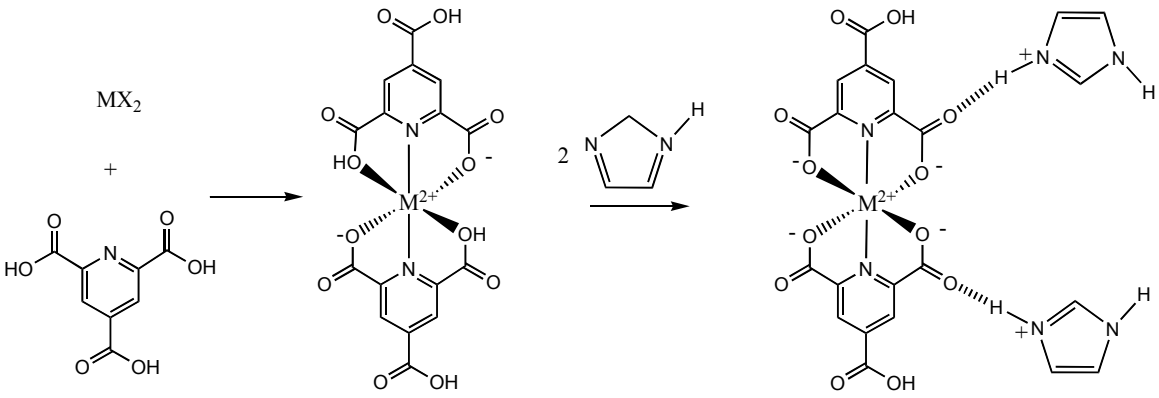


**Figure 8:** Reaction of $MX_2$ (M = Co, Ni, Cu, Zn; X = Cl or Br) with 2,4,6-pyridinetricarboxylic acid and imidazole gives the corresponding bis(imidazolium 2,4,6-pyridinetricarboxylate)metal(II) complexes (**1-4**,respectively).

We chose imidazole to link the metal-ligand complexes via hydrogen bonding. Imidazole is known to deprotonate carboxylic acids to form the corresponding imidazolium carboxylate salts.[51] We expected imidazolium bis(2,4,6-pyridinetricarboxylate) metal(II) complexes to self-assemble into layered frameworks by forming N-H···O hydrogen bonds between imidazolium cations and carboxylate groups on anions as shown in Figure 8 and 9. Accordingly, we expected that the intermolecular connectivity and spacing between cations and anions should be similar to that in layers formed by complexes of 2,6-pyridinedicarboxylic acid. Schematic representation of layers formed by Imidazolium bis(2,4,6-pyridinetricarboxylate) metal(II) complexes are shown in Figure 9.

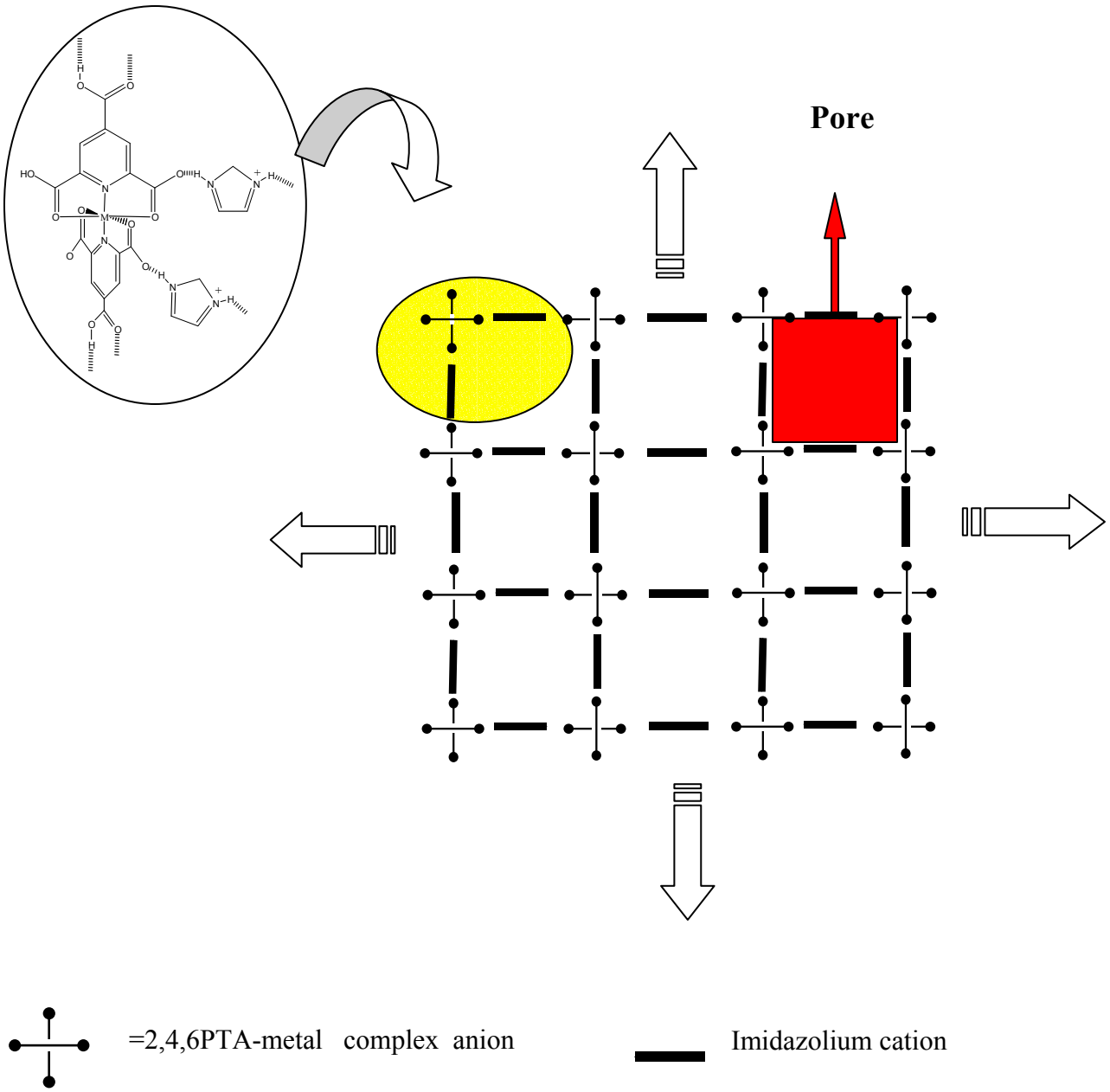


**Figure 9:** Layer framework expected to result from the formation of N-H···O hydrogen bonds in the crystal structure of bis(imidazolium 2,4,6-pyridinetricarboxylate) metal(II) salts.

We aim to show that introducing an additional carboxylic acid group at the 4-position of the pyridine ring will give an additional site for hydrogen bonding via formation of O-H···O hydrogen-bonded dimers between $CO_2H$ groups on the anions in adjacent layers. Formation of acid-acid dimers provides a significant enthalpic driving force that can cause layers to stack and align.[51] Molecular assembly in this fashion will result in formation of a three-dimensional framework of N-H···O and O-H···O hydrogen bonds that defines the bulk structure of the crystal. Overlap of pores in adjacent layers in principle will form channels that run perpendicular to the direction in which the layers stack. Our general approach to form porous materials using imidazolium bis(2,4,6-pyridinetricarboxylate) metal(II) complexes is schematically shown in Figure 10.

In order to grow these materials we needed to find a solvent system in which all the components dissolved. Synthesis of metal complexes and growth of crystals were carried out in one pot by dissolving the metal chloride or bromide salt, 2,4,6-pyridinetricarboxylic acid and imidazole in a 1:2:2 relative molar ratio in 9:1 $H_2O$:DMSO. Solutions were allowed to evaporate slowly at room temperature until crystals formed after two weeks. Crystalline materials came out of the solution after two weeks, were harvested, and X-ray diffraction data were collected on single crystals. Mixed crystals were grown using a procedure similar to that used to form crystals of pure metal complexes. Mixtures of two metal halides

were used instead of a single metal complex. Composite crystals also were formed using a procedure similar to that used for the pure metal complexes. Seed crystals of one metal complex were placed into saturated solutions of a second metal complex. Growth of epitaxial layers of the second metal complex formed on the surface of the seed crystals after one to two days. Mixed and composite crystals are described in greater detail in the sections that follow. Experimental procedures to prepare pure, mixed and composite crystals are described in detail in the experimental section.

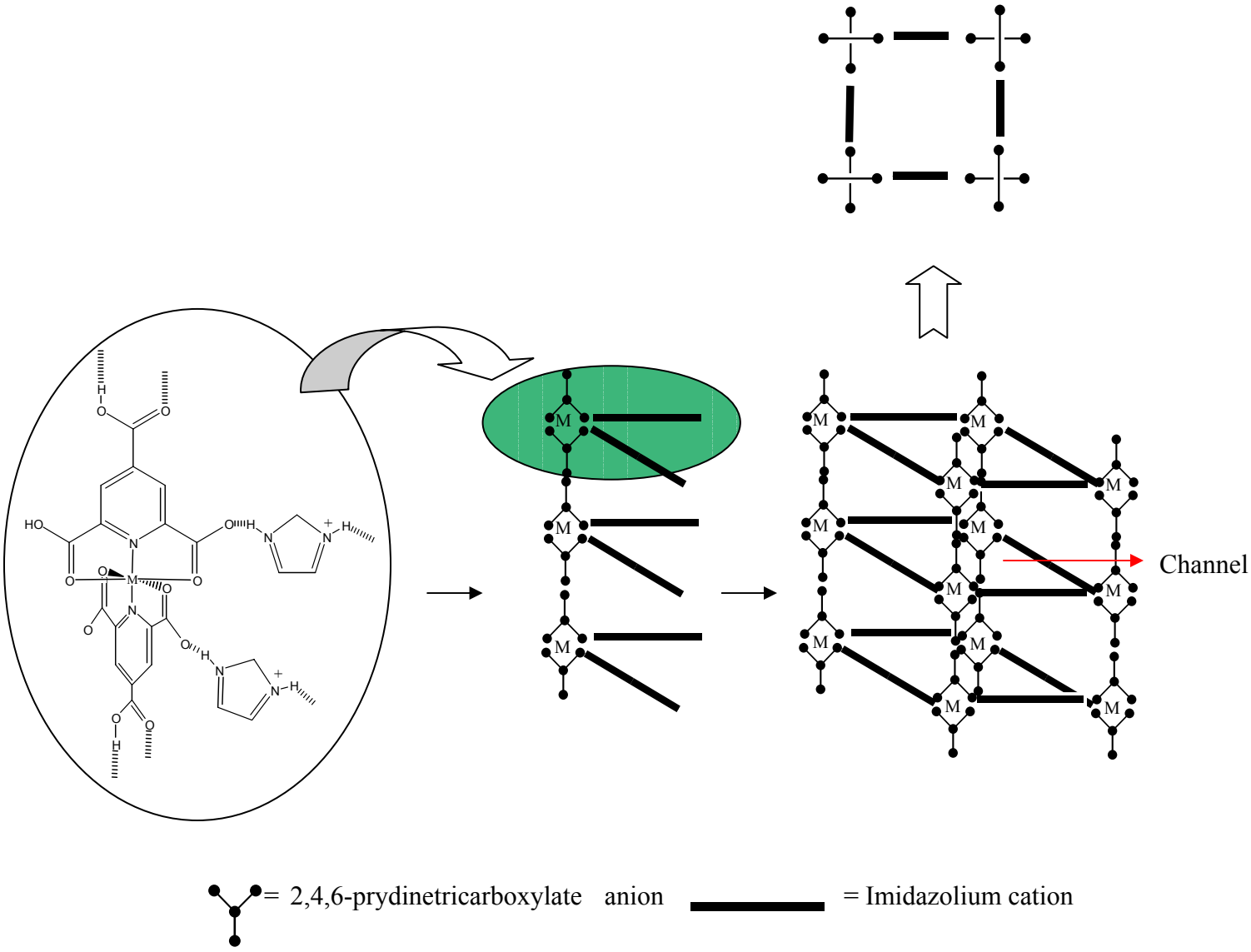


**Figure 10:** This figure describes our strategy to form a crystalline material with channels in it.

We expected molecular frameworks with open channels to crystallize with the channels either filled with molecules of solvent, or by interpenetration of a second framework within the first. Based on the size of pores from the imidazolium bis(2,6-pyridinedicarboxylate) metal(II) salts series, it is reasonable to expect that if channels form in the bis(imidazolium 2,4,6-pyridinetricarboxylate) metal(II) salts series, they will have a large enough diameter (13.7 Å x 13.7 Å in imidazolium bis(2,6-pyridinedicarboxylate) metal(II) salts) to include molecules of solvent. Alternatively, channels also may be occupied by a second framework that forms within the channel during growth of crystals. The occurrence of interpenetration can lead to a reduction in or complete elimination of void spaces within channels depending on the amount of void space occupied by the interpenetrating framework within channels. Partial interpenetration can lead to loss of porous behavior if molecules of solvent included in void spaces become trapped and are not free to move freely through channels. Molecular modeling suggests that the pores in the 2-D layers in imidazolium bis(2,6-pyridinedicarboxylate) metal(II) salts are not large enough to fit the anions of these metals complexes, but that the pores are large enough to allow imidazolium cations and carboxyl substituents on the anions to pass through. Consequently, we want determine of interpenetration competes with inclusion of solvent in channels. In the event that interpenetration occurs, we want to determine the nature of the

interactions between individual metal complexes that lead to interpenetration.

Evacuation of solvent molecules from crystals of the bis(imidazolium 2,4,6-pyridinetricarboxylate) metal(II) complexes under vacuum or heating can be expected to result in one of two different outcomes. If the 3-D hydrogen-bonded framework is robust, removal of solvent should give porous host structure with empty channels. If the 3-D hydrogen-bonded framework is not robust, removal of solvent should cause the framework to collapse and undergo a solid-to-solid phase tranformation to a new nonporous packing arrangement. We can probe porosity using thermal methods such as thermogravimetric analysis (TGA), which measures loss of mass as a functional of temperature. Samples of crystals have been examined using TGA to determine if loss of mass occurs upon heating, if the mass lost corresponds to that of integral molar amounts of solvent, and if evacuated samples that are reexposed to solvent lose. The latter experiment provides a means to determine whether our materials maintain structural integrity of the channel structure upon loss of included solvent, and whether uptake of solvent occurs into empty channels.

The thermal behavior of samples also has been examined using differential scanning calorimetry (DSC) data, which measures endo- and exothermic changes heat such as heat of fusion (melting point) and phase transitions that occur as a sample is heated. DSC provides a complementary

technique to TGA that can measure absorption of heat associated with loss of solvent molecules as well as phase transformation and decomposition of the crystal lattice.

We also have investigated the design of two novel classes of crystalline materials based on our 3-D structures. The first class of materials is single crystals that contain two or more different metal complexes that form solid solutions, or mixtures. We refer to these materials as mixed crystals. The second class of materials is single crystals composed of two different regions that contain different metal complexes. We refer to these materials as composite crystals.[25] We expect complexes of 2,4,6-pyridinetricarboxylic acid and imidazole with different metal complexes will form an isostructural series with similar molecular structures and crystal packing in a manner analogous to that of the imidazolium bis(2,6-pyridinedicarboxylate) metal(II) salts series of metal complexes. Consequently, we have investigated whether it is possible to form mixed crystals with two or more 2,4,6-pyridinetricarboxylic acid-metal complexes. We also have investigated whether it is possible to form composite crystals with two or more 2,4,6-pyridinetricarboxylic acid-metal complexes. Mixed crystals are a novel class of materials that we currently are developing in our group. These materials show promise for the design of optical materials in which properties such as color and refractive index can be manipulated based on the relative ratio of metals

present in the crystal. We also are investigating the properties of composite crystals. These novel materials have potential in the design of optical materials such as wave guides and photonic crystals that depend on deposition of thin solid films for fabrication. In addition to their novelty as materials, mixed and composite crystals provide a useful platform to probe similarity in molecular and crystal structure across a series of metal complexes. For example, success or failure in forming mixed and composite crystals provides useful information regarding the energetics involved in packing related molecular building blocks that have subtle differences in molecular structure. Composite crystals also provide a convenient system in which to probe and compare energetics at interfaces between different building blocks that have similar structures. Accordingly, we have investigated making mixed and composite crystals using different combinations of complexes **1-4**.

**Results and Discussion:**

**Layers from 2,4,6-Pyridinetricarboxylic acid, imidazole, and first-row transition metals.** We have extended the concept of using ionic hydrogen bonds to create layers of molecules from purely organic compounds to complexes that contain both organic molecules and transition metals. Specifically, we have used transition metals in the 2+ oxidation state (e.g. $Cu^{2+}$) to create coordination compounds that contain two molecules of 2,4,6-pyridinetricarboxylic acid--a ligand that binds metals at the pyridyl

nitrogen and at the two carboxylate groups--and two molecules of imidazole, Figure 8. We expected adjacent anions of the metal-ligand complexes to bind with each other via hydrogen bonding at the carboxylic acid group opposite the nitrogen atom on the pyridyl ring as shown in Figure 11.

a )

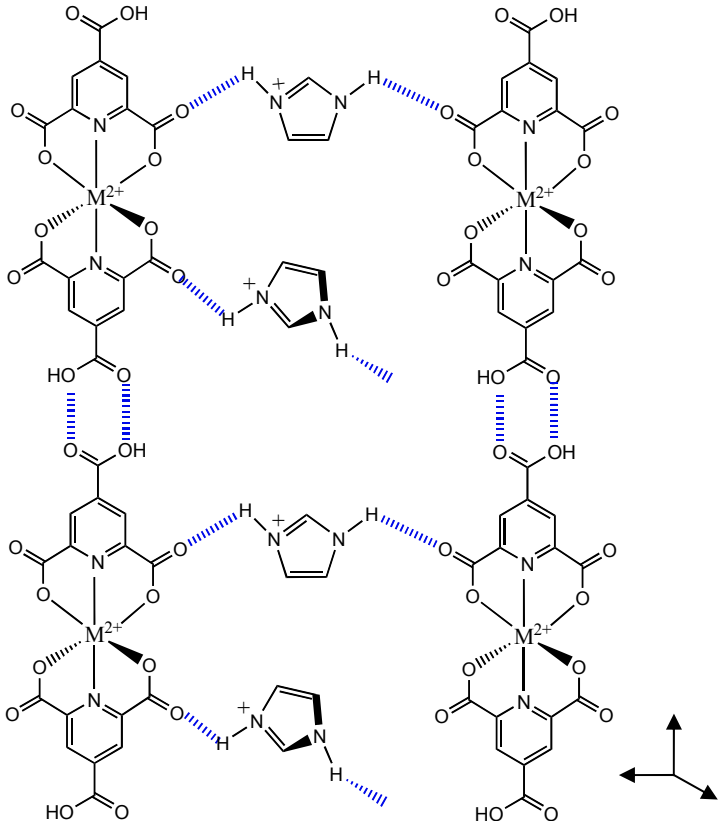

b )

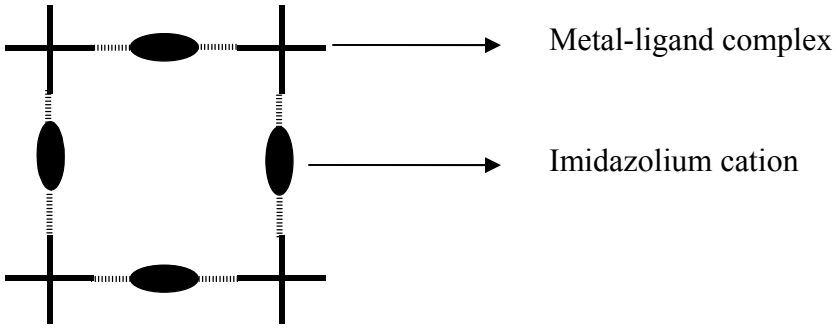


**View from top**

**Figure 11:** Anticipated orientation of +2 metal ion, 2,4,6-pyridinetri carboxylic acid and imidazole in crystal structure

These experiments tested the hypothesis that imidazole would form salts with these coordination compounds, and that these salts assemble into layers. On the basis of previous work done in our group with imidazolium carboxylate salts, we anticipated that the anions would form two sets of hydrogen-bonded chains that these chains would intersect at the anions, as shown Figure 11 to form layers. We also wanted to establish that the organic ligands would dominate crystal packing and create a host lattice that accommodates different transition metals without significantly altering crystal packing.

Reaction of 2,4,6-pyridinetricarboxylic acid and imidazole and water with $Co^{2+}$, $Ni^{2+}$, $Cu^{2+}$, $Zn^{2+}$ gives the corresponding imidazolium carboxylate metal complexes, **1-4**. These complexes form crystals in which the metal atoms are coordinated octahedrally by two ligands of 2,4,6-pyridinetricarboxylic acid. The resulting salts all contain two imidazolium cations hydrogen bonded to the dianionic metal complex and two molecules of water. These complexes readily form large crystals with well-developed faces and edges. The structures of all the complexes are very similar. Comparison of the molecular structures of the dianions shows that the geometry of the ligands on the metals varies slightly, as shown in the Figure 12**.** The N-M-N angle (M= $Co^{2+}$, $Ni^{2+}$, $Cu^{2+}$, $Zn^{2+}$) involving the nitrogen atoms on the two pridyl ligands and the central metal atom falls within the narrow range of 179.9° - 179.4°

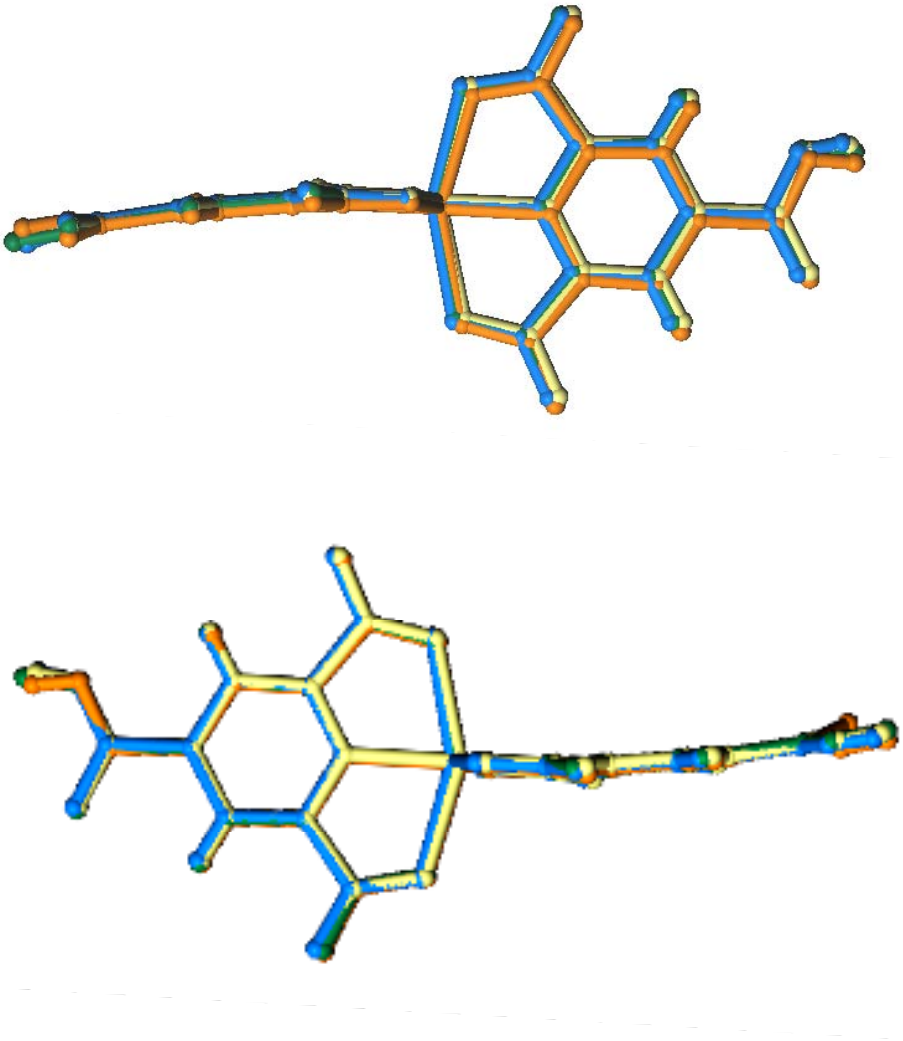

**Figure 12:** Comparison of the molecular geometries of the anions in **1-4**. Differences in structure are illustrated by the viewing the prydiyl rings from the top (a) and side (b). Cobalt, Zinc, Copper, and Nickel anion complexes are represented in orange, yellow, blue, and green, respectively

Despite minor differences in the molecular geometry of the anions, the metal complexes have similar crystal packing. All of the metal complexes crystallize in the same space group (*C*2/*c*) and have unit cells with dimensions and volumes that differ at most by 0.3 Å (1.9%) and 35.5 $Å^3$ (1.5%), respectively. The crystallographic data for complexes **1**-**4** is shown in Table 1.

TABLE 1. Collection of X-ray Data and Refinement of Crystal Structures for **1**-**4** and polmorph of Co crystal

| Compound | **1** | **2** | **3** | **4** | **Co-Polymorph** |
|---|---|---|---|---|---|
| Formula | $C_{22}H_{18}N_6O_{15}Co$ | $C_{22}H_{22}N_7O_{14}Ni$ | $C_{22}H_{21}N_6O_{14}Cu$ | $C_{22}H_{16}N_6O_{16}Zn$ | $C_{22}H_{18}N_6O_{15}Co$ |
| Molecular weight | 665.35 | 667.18 | 664.99 | 685.78 | 665.35 |
| Crystal system | monoclinic | Monoclinic | monoclinic | monoclinic | monoclinic |
| Space group | C2/c | C2/c | C2/c | C2/c | |
| Crystal | purple blocks | green prisms | blue prisms | colorless prisms | red-brown prims |
| a (Å) | 16.172(3) | 16.097(13) | 16.082(15) | 16.236(12) | 15.568(14) |
| b (Å) | 18.456(4) | 18.422(15) | 18.649(17) | 18.304(13) | 18.315(16) |
| c (Å) | 9.900(2) | 9.835(8) | 9.899(9) | 9.9220(7) | 9.895(9) |
| $\alpha$ (°) | 90 | 90 | 90 | 90 | 90 |
| $\beta$ (°) | 112.172 | 111.61(10) | 112.3(10) | 111.971(10) | 104.446(2) |
| $\gamma$ (°) | 90.0 | 90 | 90 | 90 | 90 |
| V ($Å^3$) | 2736.4(10) | 2711.3(4) | 2746.8(4) | 2734.6(3) | 2732.0(4) |
| Z | 4 | 4 | 4 | 4 | 4 |
| $D_{calc}$ ($g/cm^3$) | 1.615 | 1.634 | 1.608 | 1.666 | 1.618 |
| F(000) | 1356 | 1372 | 1360 | 1392 | 1356 |
| $\mu$(Mo–$K_\alpha$) ($mm^{-1}$) | 0.713 | 0.801 | 0.879 | 0.989 | 0.714 |
| Temperature (K) | 568(2) | 200(2) | 298(2) | 200(2) | 200(2) |
| $\theta$–2$\theta$ scans; $\theta$ range (°) | 1.75-28.36 | 1.75-28.22 | 1.75-28.26 | 1.75-28.30 | 1.35-28.29 |
| Reflections collected | 3195 | 3177 | 3235 | 3198 | 6352 |
| Parameters | 200 | 191 | 200 | 206 | 424 |
| Data/parameters (obs refl) | 15.97 | 16.54 | 16.17 | 15.51 | 14.98 |
| $R/wR^2$ (obs data)[a] | 0.052/0.141 | 0.045/0.112 | 0.049/0.1432 | 0.042/0.114 | 0.051/0.128 |
| $R/wR^2$ (all data)[a] | 0.058/0.145 | 0.053/0.107 | 0.057/0.1493 | 0.049/0.118 | 0.093/0.147 |
| S | 1.056 | 1.060 | 1.108 | 1.089 | 1.067 |

[a] $R = \Sigma(||F_o|-|F_c||)/\Sigma|F_o|$; $wR^2 = [\Sigma w(|F_o|-|F_c|)^2/\Sigma w(F_o)^2]^{1/2}$

Packing in these solids is dominated by hydrogen bonding between imidazolium cations and carboxylate anions. Anions of the metal complex are joined to imidazolium cations by ionic $^{+}$N-H···O$^{-}$ hydrogen bonds as anticipated shown in Figure 13. The four carboxylate groups of the anions are oriented in a flattened tetrahedral arrangement around the metal, as shown in Figure 13. Two metal-anion complexes are joined together via hydrogen bonding between $CO_2H$ groups at the para position of the pyridyl ring as shown in Figure 14. We expected to see O-H···O hydrogen-bonded dimers involving two O-H···O hydrogen bonds between $CO_2H$ groups on the anions in adjacent layers; instead, formation of a single O-H···O hydrogen bond is observed. Consequently, each anion participates in the formation of two perpendicular chains of $^{+}$N-H···O$^{-}$ hydrogen bonds that intersect at the anions. The resulting network of cross-linked chains forms interpenetrated layers. This interpenetration decreases the size of the empty space in the channels. A view of a channel from the crystal structure of **4** is shown in Figure 15. The hydrogen-bonded layers formed in crystals of **1-3** are essentially identical in structure to those in **4** and are not shown**.**

The surface of a single hydrogen-bonded layer **4** (and **1**-**3** and **5**) is not flat but corrugated. Each layer forms a grid of cations and anions that contains cavities between the ions; the distance between metal atoms is 13.7 Å by

13.7 Å along the edges of the grid, and 19.9 Å by 18.3 Å along the long and short diagonals of the grid, respectively, as shown in Figure15. The cavities are not empty in the crystal, but instead are filled by interpenetrated layers as shown in Figure 16. Molecules appear to pack in wavy layers rather than flat layers in order to accommodate interpenetration, as shown in Figure 16. The fact that the cavities are large enough to accommodate aromatic rings is an attractive feature that suggests that channels should be able to trap guest molecules with aromatic structures if interpenetration can be prevented. A view looking down the *a* axis (100 face) of two layers stacked in this manner is shown in Figure 17. Views of crystal packing looking down the *b* axis (010 face) and *c* axis (001 face) are shown in Figure 18 and 19, respectively. These structural features are consistent in all four structures. Given the range of sizes and electronic structures of Co, Ni, Cu, and Zn, these data suggest that supramolecular frameworks of this type are likely to form for other transition metals in the 2+ oxidation state as well.

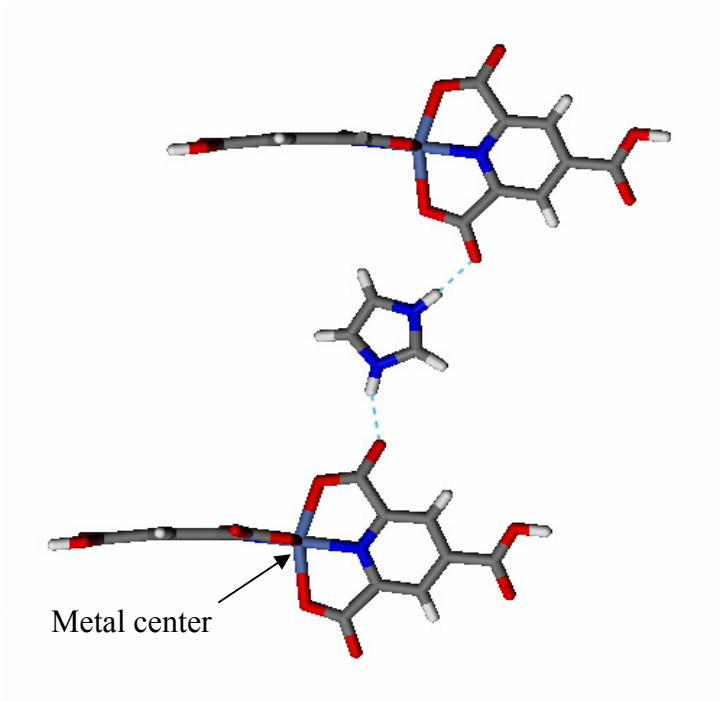


**Figure 13:** Metal-ligand anion complexes are joined to imidazole cations via hydrogen bonding. The metal ion (purple color) is placed in the metal-ligand anion in such an arrangement that four carboxylate groups of the anions are oriented tetrahedrally around it.

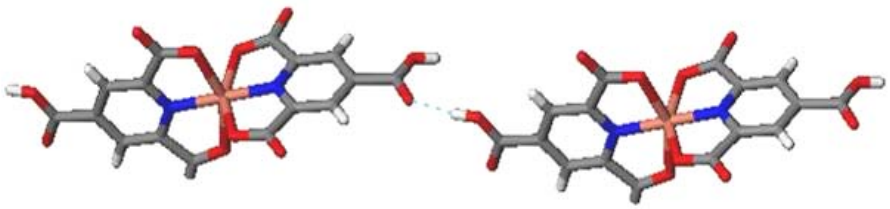

**Figure 14:** Hydrogen bonding between metal-ligand complex through carboxylic group at fourth positioned Carbon atom at pridyl group.

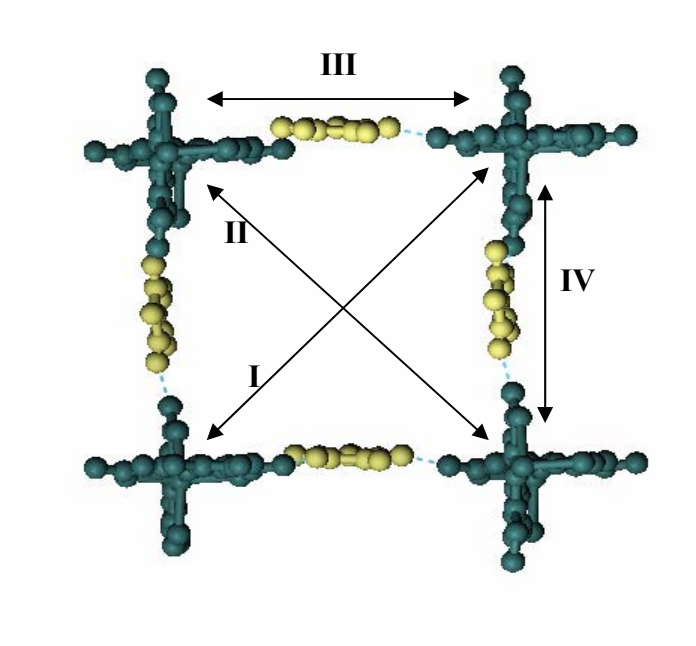


**Figure 15:** Top view of a channel of Zn complex (100 face) is shown. Metal-ligand anion complexes are represented by green color, imidazole cations are represented by yellow color. Dimensions of the cavity and spacing of the metal atoms within a layer are indicated by arrows **I-IV**

which correspond to the following disteances: I, 19.85 A; II, 18.30 A; III, 13.71 A; IV, 13.71 A

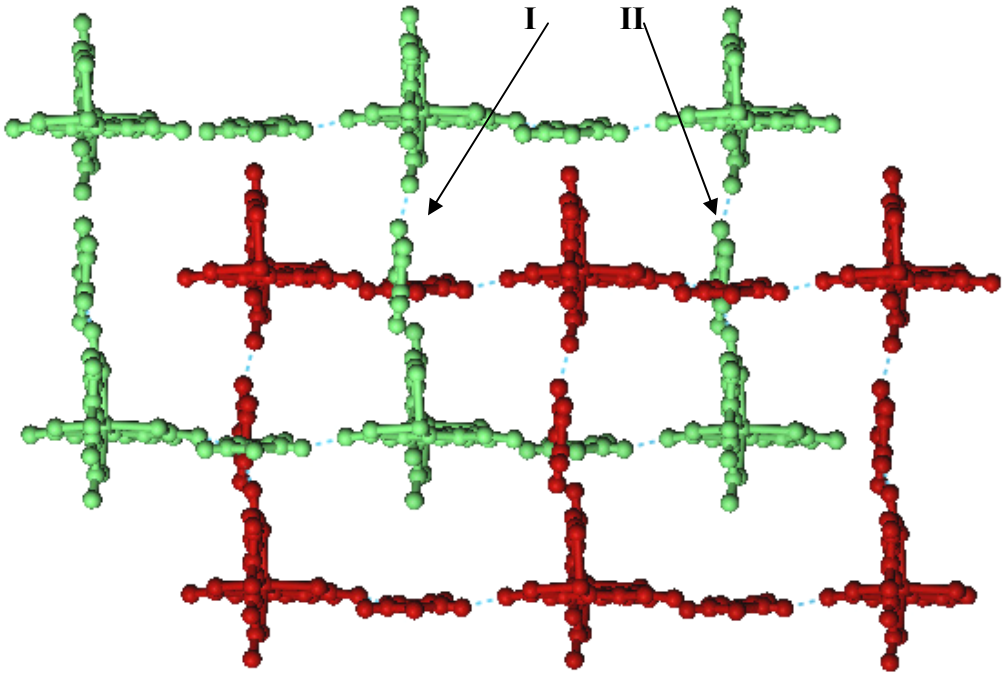


**Figure 16:** Interpenetrated layers are shown. Green layer is above red layer as shown by arrow **I**, but next adjacent green unit cell goes under red layer as shown by arrow **II** and so on so far.

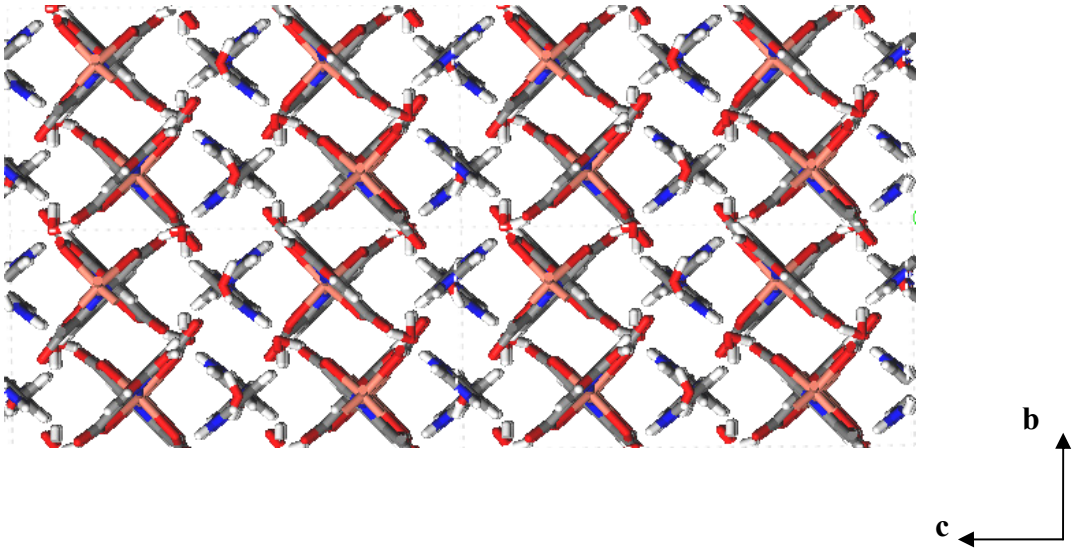


**Figure 17:** View of the 100 face of Cu crystals.

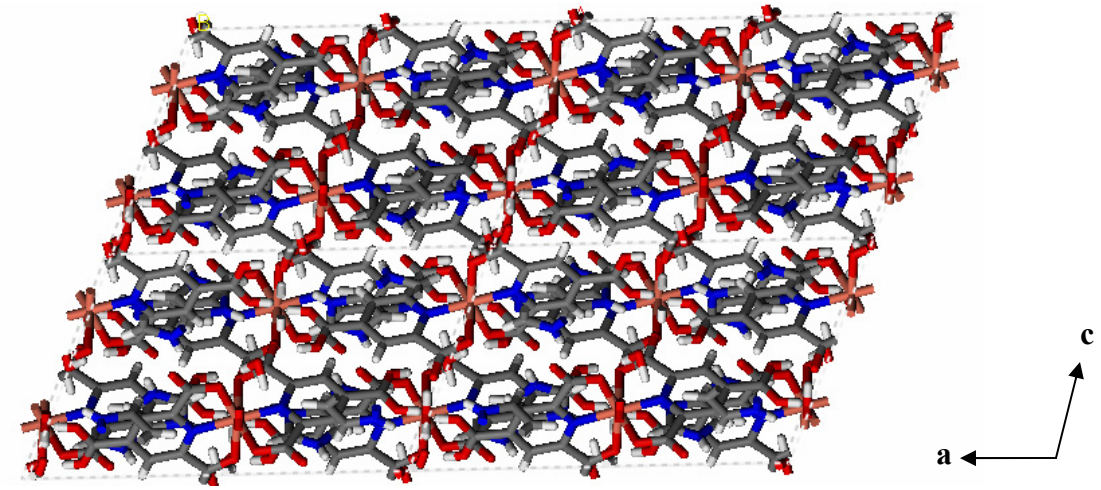


**Figure 18:** View of the 010 face of Cu crystals.

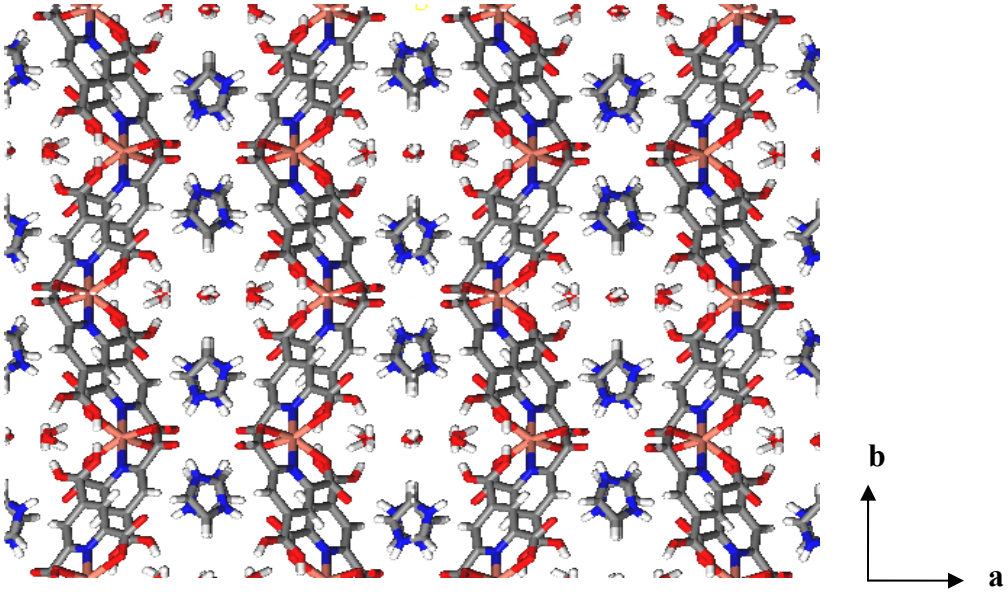


**Figure 19:** View of the 001 face of Cu crystals.

Growth of all crystals was achieved by evaporation of solutions of 9:1, $H_2O$:DMSO mixture that were left open to the atmosphere. Clear, colored crystals shaped like parallelograms formed after about two weeks.

It should also be noted that trigonal shaped crystals for the Co complex appeared briefly in solution prior to the parallelograms. These trigonal shaped crystals dissolved after several days, with subsequent appearance of the parallelograms within one day. Trigonal crystals of the Co complex were harvested for structural analysis. Illustrations of first and second types are shown in Figure 20. The X-ray crystal structure of one of these crystals showed that it is a polymorph with similar molecular structure and crystal packing to that of the parallelogram form. Crystals of the Ni and Cu complexes with similar trigonal morphology also formed. They appeared in the solution in about a week and then disappeared in a day or two. The similar morphology of those crystals to that of the Co polymorph suggests that the Ni and Cu complexes both form a second polymorph as well. The crystal shaped like a parallelogram appears to be more stable than the trigonal crystals because the trigonal crystals dissolved before the first type formed in the solution. This behavior is consistent with the formation of a less stable crystal form (i.e., trigonal) that nucleates and comes out of solution first, followed formation of a more stable crystal form (parallelograms) that subsequently nucleates and comes out of solution last. Crystallization under thermodynamic conditions in which

growth and dissolution of crystals is reversible should yield crystals with the most stable crystal lattice—that is, with the most efficient packing that maximizes favorable contacts between molecules. Slow evaporation can lead to nucleation and growth of crystals under both thermodynamic or kinetic conditions. The fact that the trigonal crystals grow and then dissolve suggests that formation of the trigonal polymorph occurs under thermodynamic conditions. Dissolution of the trigonal form can be explained if crystals of the more stable parallelograms nucleate in the same solution, causing crystals of the less stable trigonal form to dissolve and provide solute for the growth of the parallelograms.

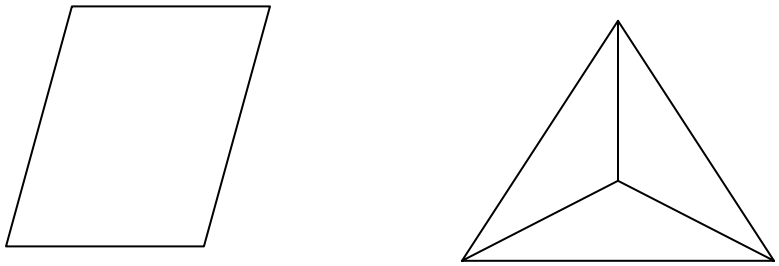

**Type 1** **Type II**

**Figure 20:** Type I (on the left) and Type II (on the right) are observed polymorphs in growing the Co crystals.

**Mixed Crystals.** The similarity between crystal packing in structures containing 2,4,6-pyridinetricarboxylic acid, imidazole, and 2+ transition metals ($Co^{2+}$, $Ni^{2+}$, $Cu^{2+}$, and $Zn^{2+}$) suggested that the hydrogen-bonded network of organic ligands would serve as a host lattice in which one metal could be replaced by another metal without disturbing the lattice. This type of material, which we refer to as a mixed crystal, contains a mixture of two or more different types of transition metals within the same crystal. Mixed crystals represent a new class of materials that should exhibit properties that can be altered systematically as a function of the types and relative ratios of transition metals that are present. Manipulation of physical properties in this manner is analogous to the manner in which the conductivity of semiconductors is modulated by doping. Moreover, mixed crystals should have properties such as index of refraction and color that can be controlled with a high degree of predictability and precision.

To test the hypothesis that one transition metal can be substituted by another without significantly altering the crystalline lattice, we grew crystals from a series of solutions that contained complexes with two different metals, $M_1$ and $M_2$, where $M_1$ and $M_2$ were different combinations of $Co^{2+}$, $Ni^{2+}$, $Cu^{2+}$, and $Zn^{2+}$. The composition of the solutions is 50 mol % of $M_1$ and 50 mol % of $M_2$. Also the composition of 33.3 mol % of $M_1$, 33.3 mol % of $M_2$, 33.3 mol % of $M_3$ is tested. We anticipated that crystals grown from these solutions would incorporate the metal complexes in the same relative ratios that were present in solution.

In addition, we expected that the color of the crystals would change as types of metals are changed. Results from using this technique to grow different mixed crystals are shown in Figure 21.

Pure crystals are shown in Figure 22. The crystal in Figure 23 illustrates how mixing the blue Cu complex (**3**) with the green Ni complex **(2)** produced a mixed crystal that is a light green color. Other examples of mixed crystals are shown in Figure 24, 25. We also have grown one example of a crystal with three components that contained equimolar amounts of the Co, Ni, and Cu complexes (Figure 26).

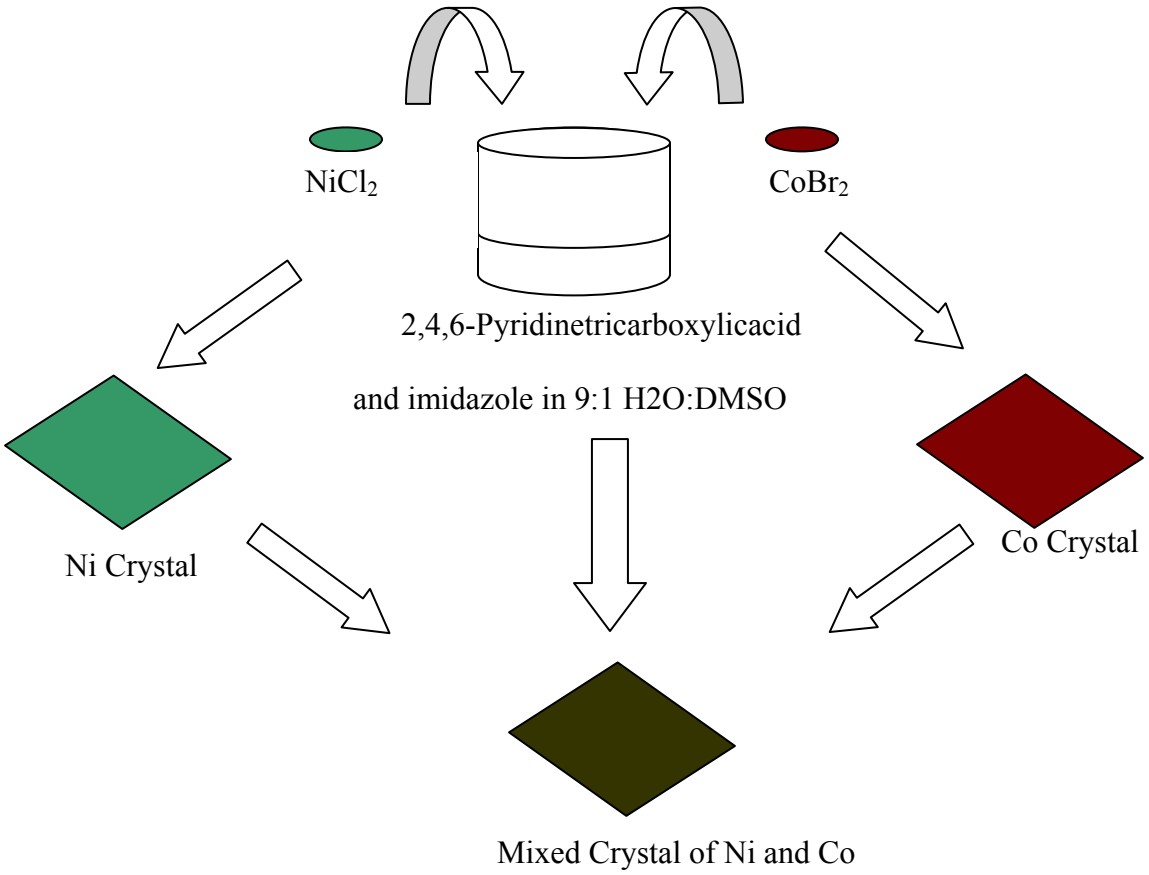


**Figure 21:** Illustration of a hypothetical mixed crystal (dark green) grown from a solution that contains complexes of both Ni (green) and Co (red).

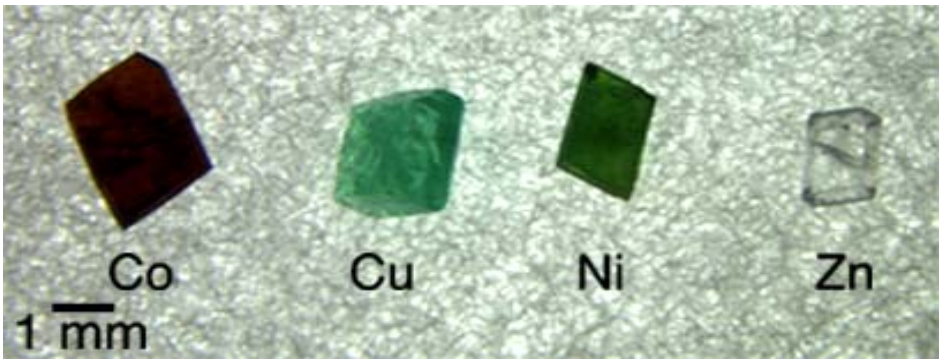


**Figure 22:** Pictures of crystals of Co, Cu, Ni and Zn complexes are shown.


**Figure 23:** Mixed crystals of 1:1 **Cu : Ni**.

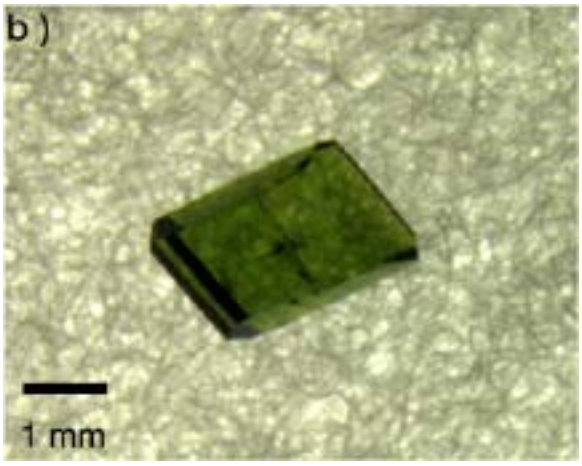


**Figure 24:** Mixed crystals of 1:1 **Co : Ni**

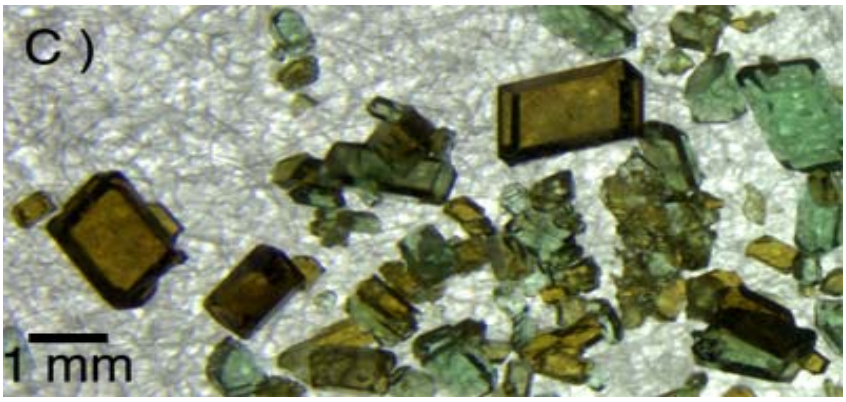


**Figure 25:** Mixed crystals of 1:1 **Co : Cu**

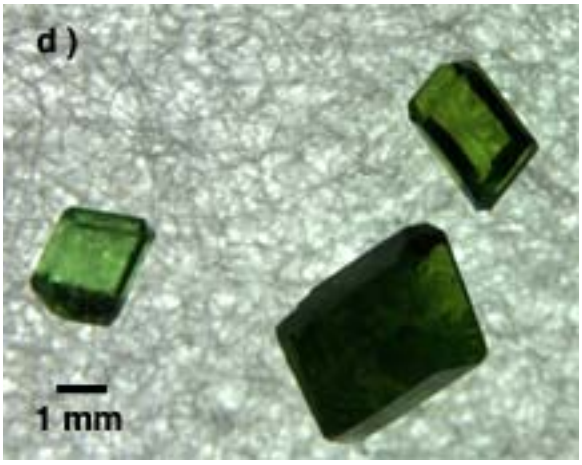


**Figure 26:** Mixed crystals of 1:1: 1 **Co : Ni : Cu**

As described in the Experimental Section, synthesis and crystallization of pure **1**-**4** was carried out in one pot by mixing 2,4,6-pyridinetricarboxylic acid, imidazole, and a metal halide salt in 9:1 DMSO:$H_20$ mixture in a 2:2:1 relative molar ratio, respectively, followed by crystallization of these complexes by slow evaporation from the same solution. The resulting metal complexes contained 2,4,6-pyridinetricarboxylic acid, imidazole, and a metal salt in DMSO in a 2:2:1 relative molar ratio, respectively. Mixed crystals were grown using this same technique by dissolving a mixture of two different metal halide salts instead of a single metal halide salt. Since the rate at which the metal complexes form varies for different metals, it is possible that the ratio of different metal complexes incorporated into a given mixed crystal may vary depending on the rate at which crystals nucleate and grow. For example, consider the case in which a complex with one metal, $M_1$, forms at a faster rate than a complex with a second metal, $M_2$. If crystals of $M_1$ begin to nucleate and grow at a rate that is fast relative to the formation of $M_2$ in solution, the crystal should incorporate a higher percentage of $M_1$ relative to $M_2$. If crystals of $M_1$ nucleate and grow at a rate that is comparable to or slower than the formation of $M_2$ in solution, the crystals should incorporate $M_1$ and $M_2$ statistically as a function of the relative molar ratio of $M_1$ and $M_2$ introduced into the solution.

**Composite Crystals.** Growth of thin films of materials is one of the more important and fast growing areas of research in the development of a wide

range of materials (e.g., liquid crystals, polymers, coatings, optical waveguides, and magnetic media). We are working to develop a technique to make single-crystal films based on our layered metal complexes. Our approach takes advantage of the close structural match between the lattices in the crystals of **1**-**4**. A crystal of one metal complex as a substrate, or seed, was used to nucleate and grow a layer of a different metal complex epitaxially on the surface. This concept is illustrated in Figure 27 and Figure 28. Different examples of composite crystals composed of two different metal complexes are shown in Figure 29-33. These crystals formed when seed crystals of the cobalt complex (**1**) were placed into a solution in 9:1 DMSO:$H_20$ mixture that contained either the Ni complex (**2**) or the Cu complex (**3**). Epitaxial growth of a new layer on the seed crystal of **1** produced composite crystals with fast, uniform growth of an outer layer of **2** or **3** on the seed crystal of **1** in Figure 27 and 28. The morphology and aspect ratio of the crystalline material that forms the epitaxial regions of the composite crystal are commensurate with those of the underlying seed crystals. Although it is demonstrated that epitaxial deposition of just one new layer of a different complex, we are working to develop a technique to grow many successive crystalline layers that contain different metals. Optical polarizing microscopy showed that the inner and outer regions of these composite crystals extinguish light uniformly under crossed polarizing lenses. This behavior indicates that

composite crystals behave as single crystals rather than as a mosaic of two different, or twinned, crystals that have different orientations.

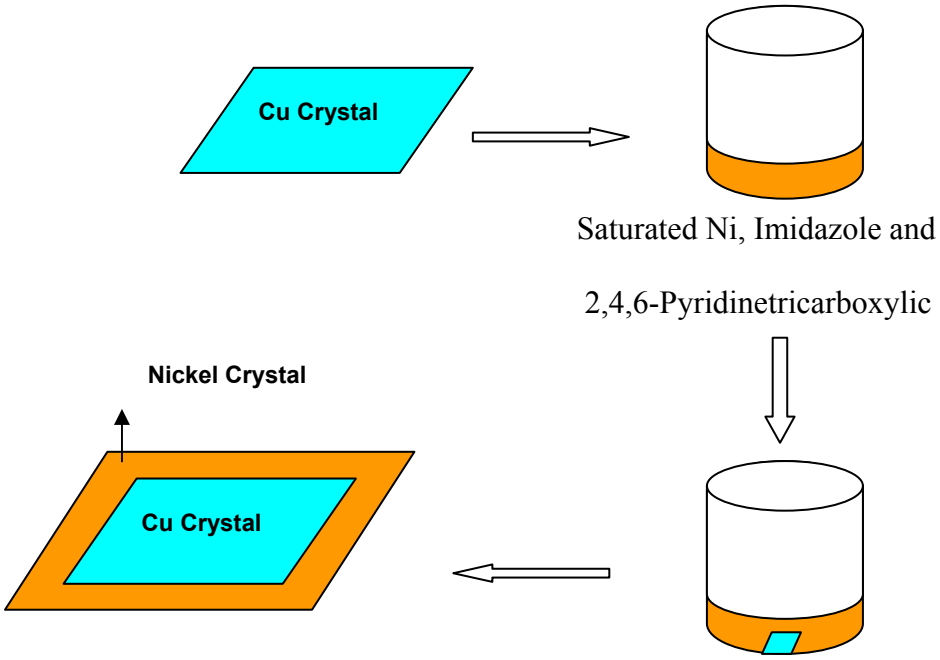


**Figure 27:** Illustration of a hypothetical composite crystal in which nickel crystal is grown as a layer on the surface of copper crystal.

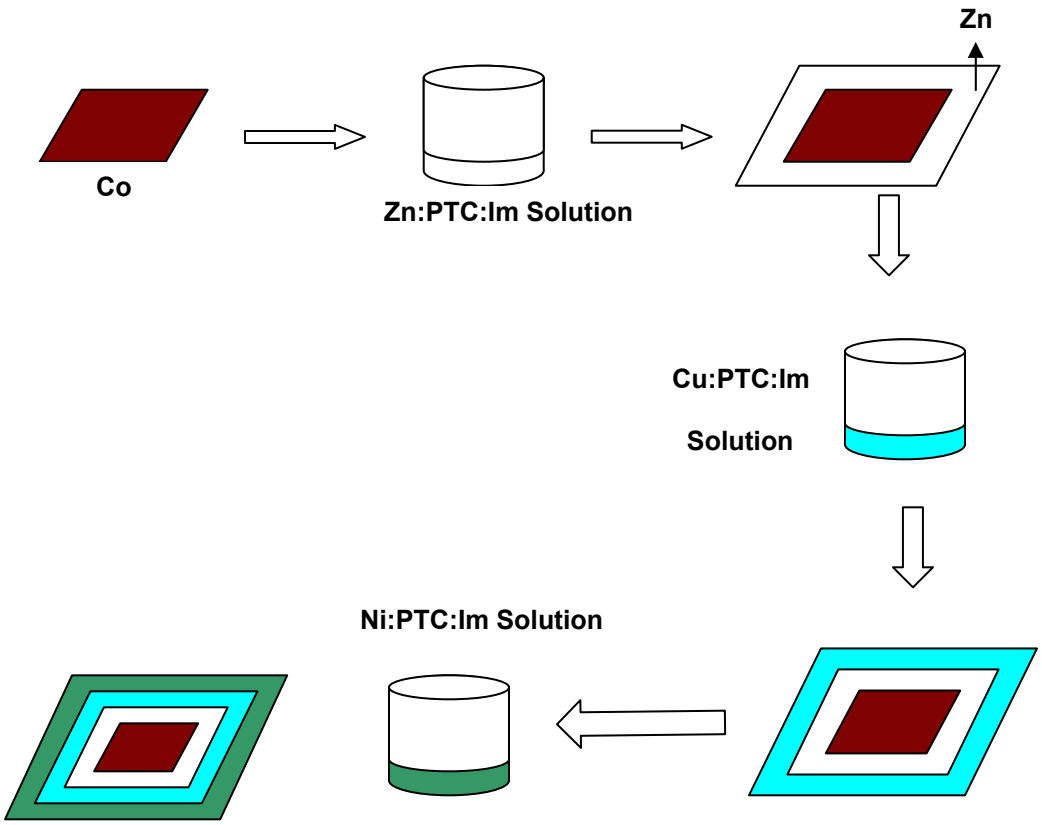


**Figure 28:** Illustration of a hypothetical composite crystal in which successive layers of different metal complexes are added sequentlly to the surface of a seed crystal

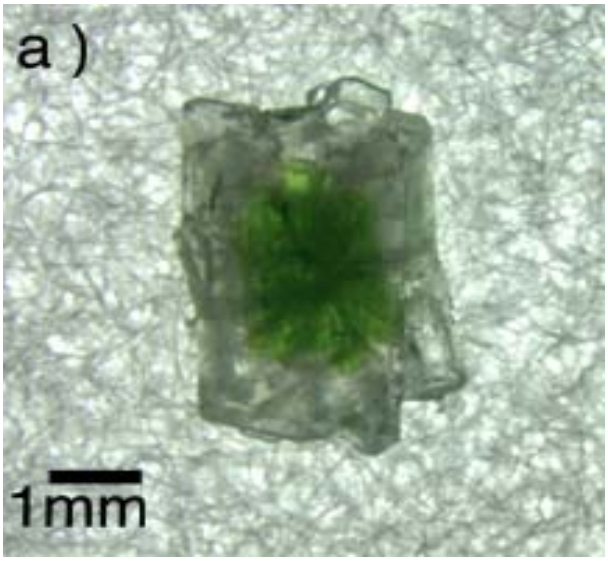


**Figure 29:** A composite crystal composed of an inner region of Ni (**2**) and outer region of Zn (**4**)


**Figure 30:** A composite crystal composed of an inner region of Co (**1**) and outer region of Ni (**2**)

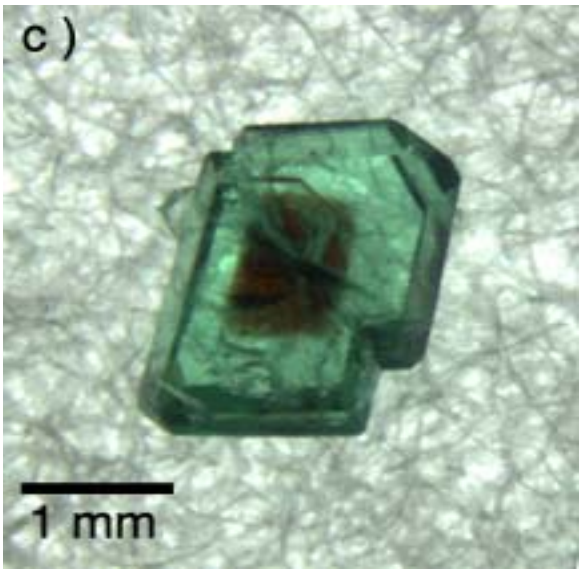


**Figure 31:** A composite crystal composed of an inner region of Co (**1**) and outer region of Cu (**3**)


**Figure 32:** A composite crystal composed of an inner region of Ni (**2**) and outer region of Cu (**3**)

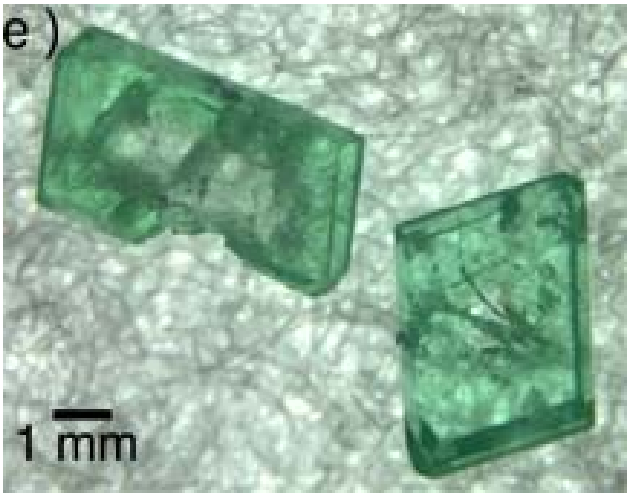


**Figure 33:** A composite crystal composed of an inner region of Zn (**4**) and outer region of Cu (**3**)

**Thermogravimetric Analysis TGA) and Differential Scanning Calorimetry (DSC),** TGA data measures the loss of mass in a sample as a function of temperature. We collected TGA data of compounds **1-4** that is consistent for all four complexes. TGA plots for samples of **1-4** show that there is a weight loss of 2 % of crystal weight upon heating from 80 °C to 120 °C. Loss of this relative mass is correlates well with the weight of water contained in the mass of the crystals in the samples. These results show that heating drives all of the water out of the lattice. The TGA plots show that decomposition occurs after 250 °C, as seen in Figure 34. The anhydrous form of Cu complex was obtained by heating a sample of crystals up to 120-130 °C. The resulting polycrystalline samples was then placed in a vial open to atmosphere to allow it to reabsorb water from air. After one week, we recollected TGA data on this solid (Figure 36) and found that there was no weight loss between 90-120 °C. These results show that the anhydrous form of Cu complex did not absorb water from air over seven days. TGA plots of anhydrous samples placed in contact with liquid water similarly showed no uptake of water by the sample.

Differential Scanning Calorimetry (DSC) plots show either two or three endothermic peaks, as shown in Figure 35. The first peak correlates with loss of water in the TGA plots. The peaks correspond to the decomposition of the crystals. DSC also was used to monitor loss of water

and subsequent readsorption of water from an sample of the Zn complex using the same procedure as that used with TGA. The DSC plot for a sample of the anhydrous Zn complex obtained after exposure to the atmosphere for on week shows no endothermic peak for loss of water (Figure 41). This result supports the conclusion from the TGA data that once water is removed from crystals of the metal complexes, the resulting anhydrous samples do not readsorb water. TGA and DSC plots of **1-4** are shown in Figures **34**-**41**. DSC and TGA plots for **1**-**4** show similar thermal behavior.

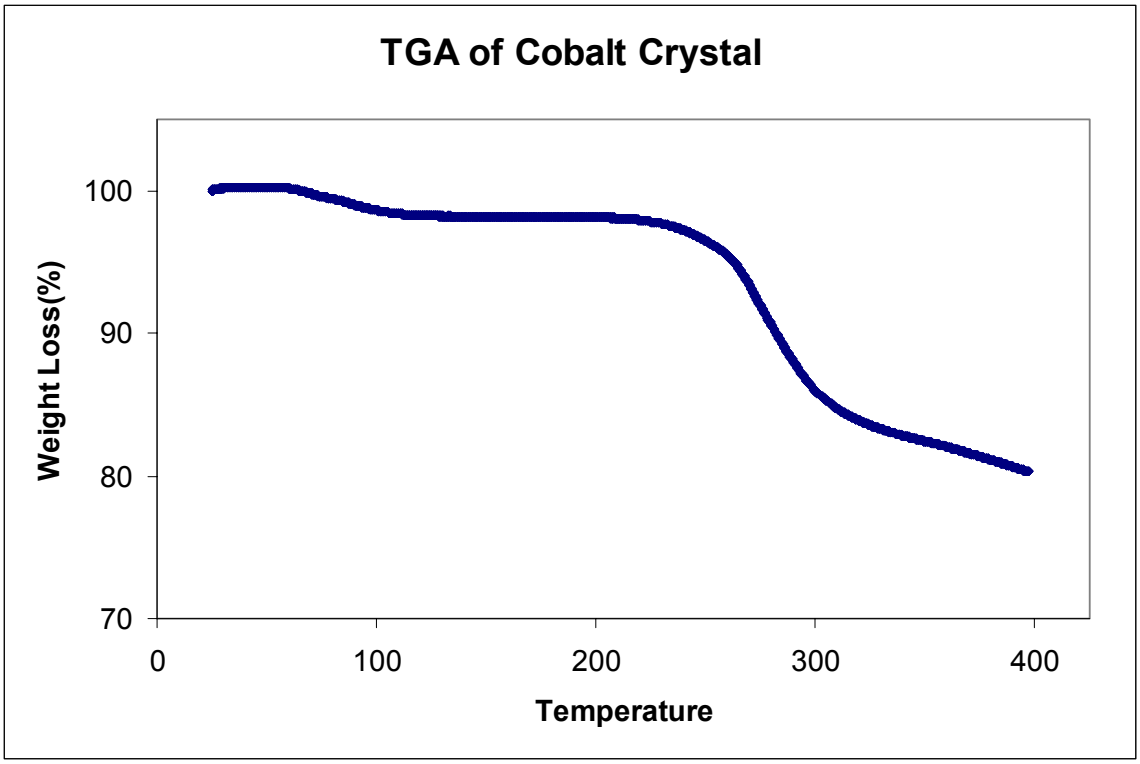


**Figure 34:** TGA plot of Co (**1**) crystal. First weight loss suggests that water is lost between 80 C and 120 C.

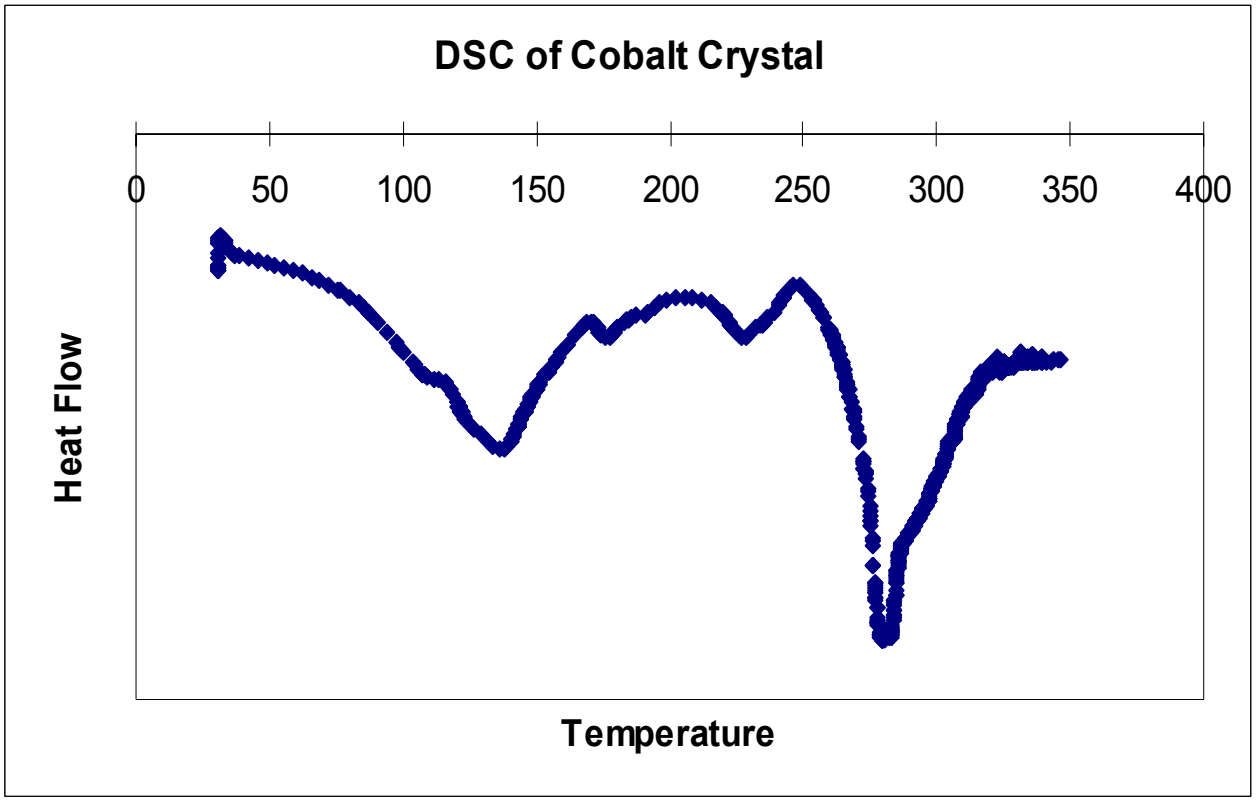


**Figure 35:** DSC plot of Co (**1**) complex. First peak corresponds to weight loss of water molecule in the lattice. Last peak most likely to corresponds to decomposition of complex.

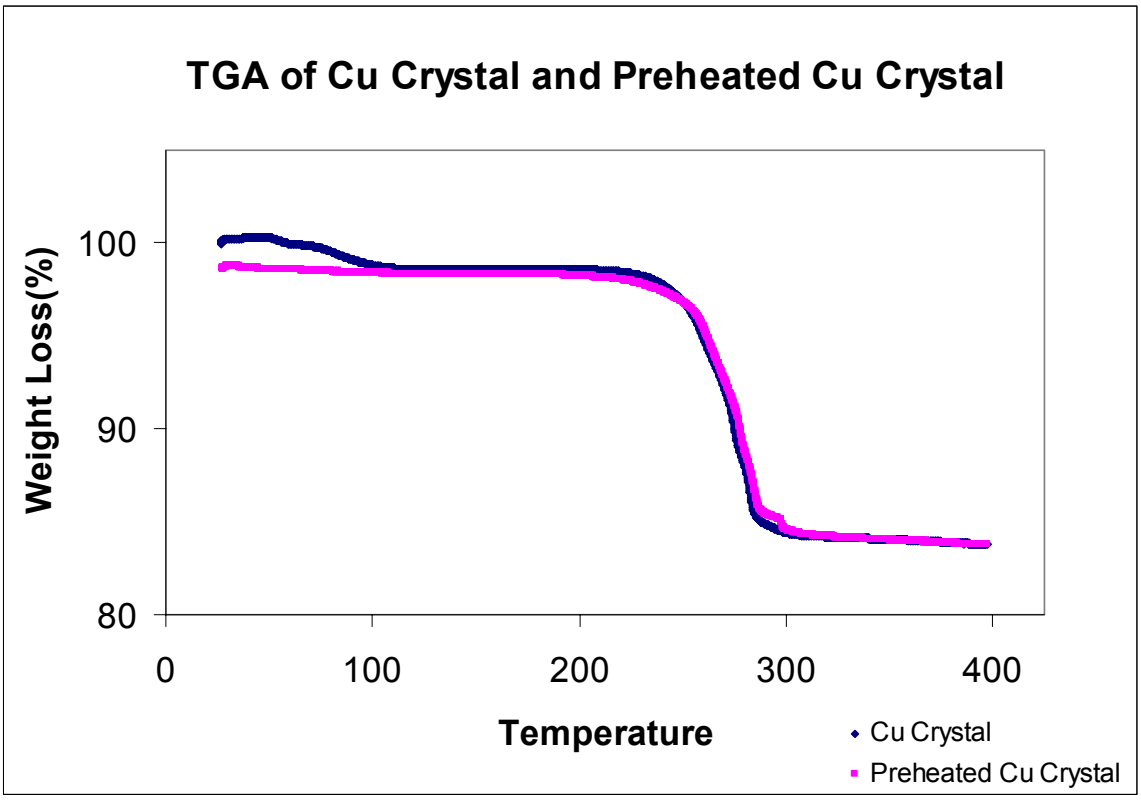


**Figure 36:** TGA plot of Cu (**3**) and Cu complex which was heated to 120 C previously. These two superimposed TGA plots suggest that water molecule can not take place in the lattice once it is lost via heating.

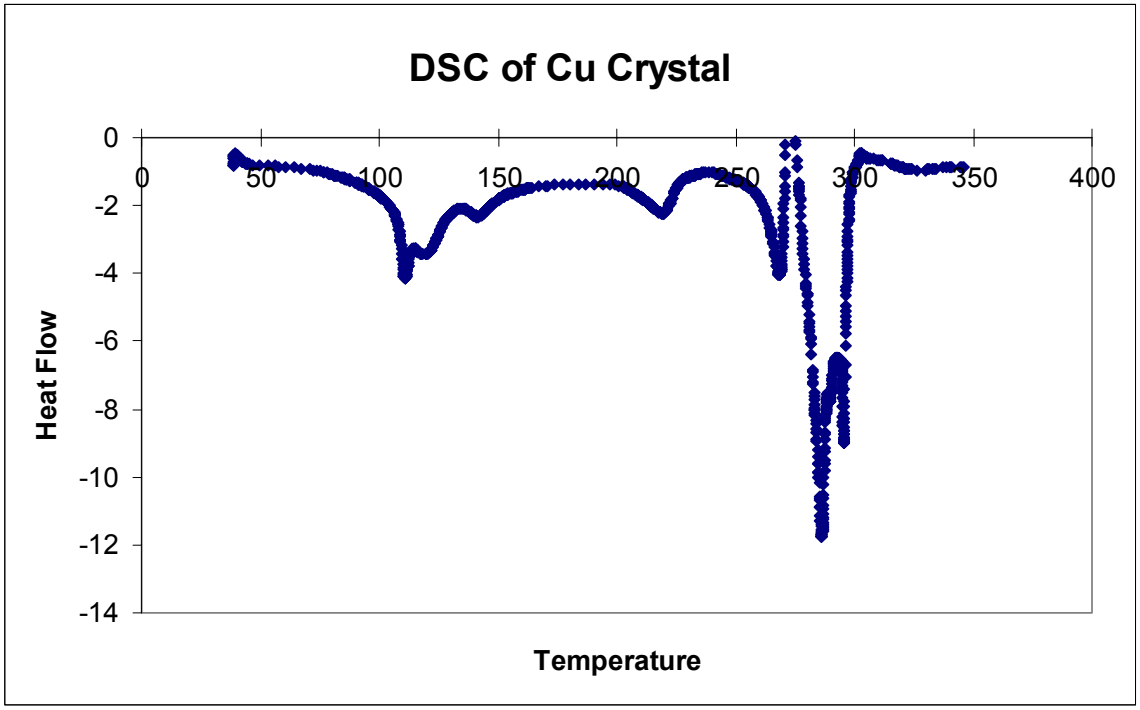


**Figure 37:** DSC plot of Cu (**3**) complex.

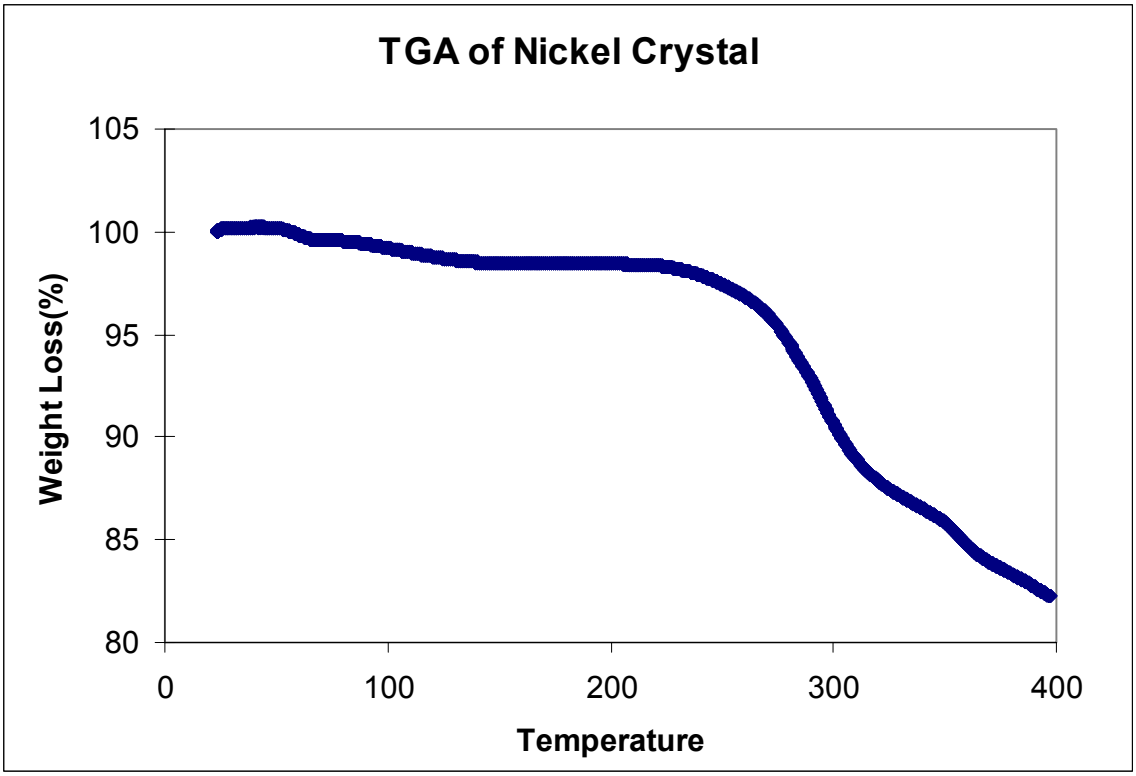


**Figure 38:** TGA plot of Ni (**2**) complex.

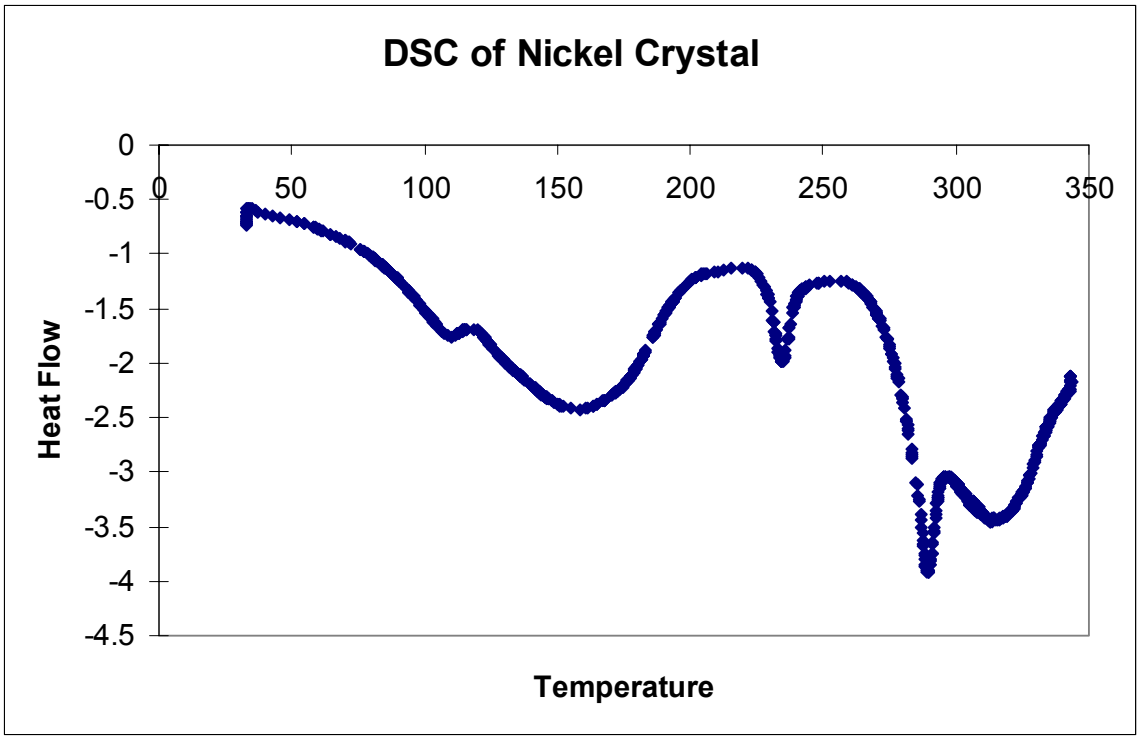


**Figure 39:** DSC plot of Ni (**2**) complex.

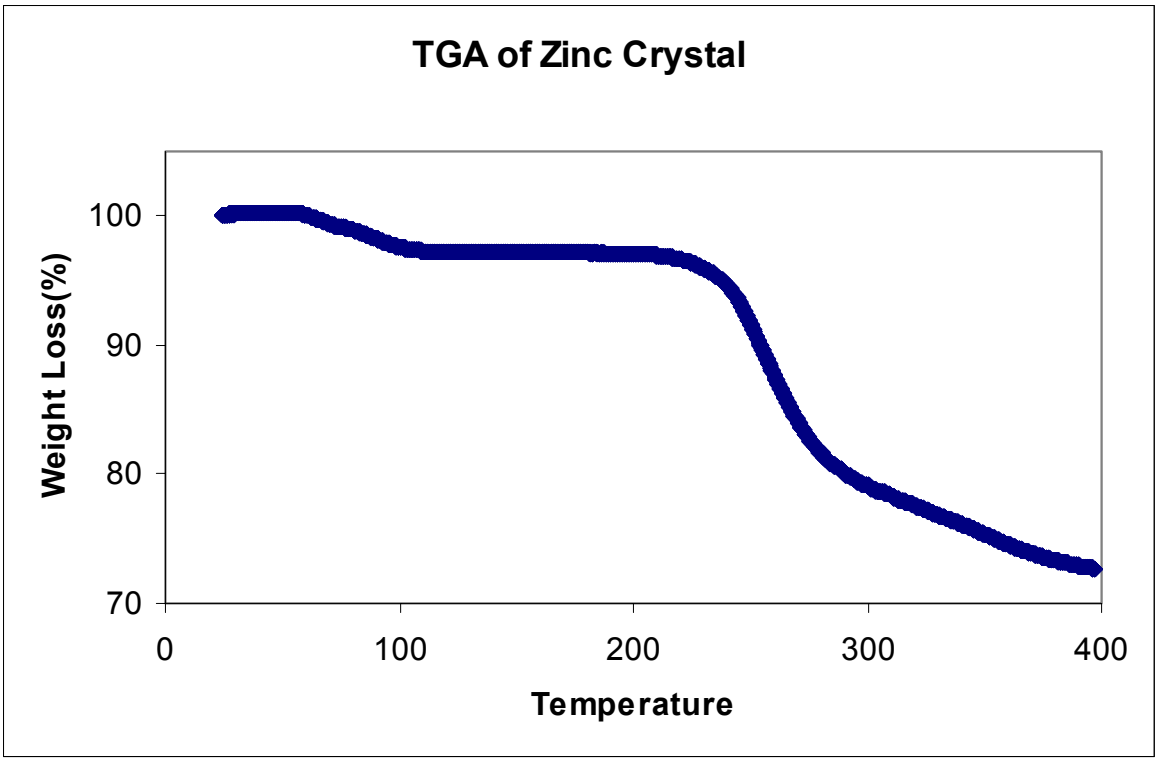


**Figure 40:** TGA plot of Zn (**4**) complex.

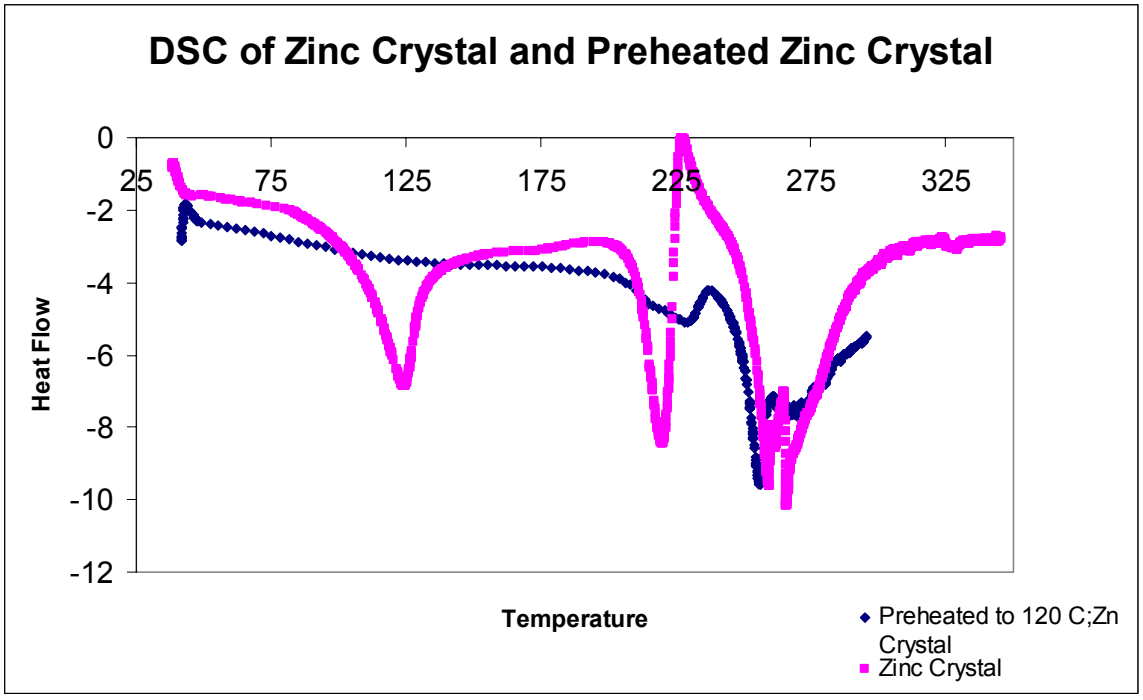


**Figure 41:** DSC plots of Zn (**4**) complex and Zn (**4**) complex which was heated to 120 C previously are shown. These two superimposed plots suggest that first peak corresponds to loss of water which is not present in DSC plot of preheated Zn (**4**) complex. Last two peaks most likely to due to decomposition of complex.

**Conclusion:** We have shown that bis(imidazolium 2,4,6-pyridinetricarboxylate)M(II) complexes **1-4** serve as supramolecular building blocks that form extended layers that have a single, well-defined, predictable structure in the solid state. These layers pack in a predictable arrangement to form a persistent 3-D network that accommodates at least four different transition metals without significantly altering molecular packing. Although, interpenetration of two independent frameworks prevents open channels from forming, the crystal structure still has channels with reduced void space that includes molecules of water during crystallization. Consequently, this 3-D framework serves as a platform with which to control molecular packing by design for engineering the structures, and, ultimately, the properties of crystals. We have demonstrated that hydrogen bonding can be used successfully to control assembly of molecules. The crystalline solids of **1-4** represent a new class of modular materials in which the organic ligands serve as a structural component that defines a single packing arrangement that persists over a range of structures, and in which the metal serves as an interchangeable component. This type of supramolecular modularity is a crucial element for engineering useful materials because it provides a handle with which to alter the physical properties of a material without changing the structure of the material. This concept is analogous to the way in which the properties of copolymers are modified at the molecular level by altering the molecular structure of just one of a pair of monomeric starting

materials. We have demonstrated the utility of this modular approach at the supramolecular level through the design of mixed and composite crystals.

## Experimental

**General Techniques.** Cobalt (II) bromide, nickel (II) bromide, copper (II) bromide, zinc (II) bromide, imidazole and 2,4,6-trimethylpyridine were purchased from Aldrich or Acros. 2,4,6-Pyridinetricarboxylic acid was synthesized by oxidation of 2,4,6-trimethylpyridine with $KMnO_4$. All chemicals were used as received without further purification. IR samples were prepared as powders. IR spectra were obtained in a Nexus 870 FT-IR 360 instrument with an ATR accessory. Melting point data were collected with a Meltemp instrument and are uncorrected. Differential Scanning Calorimetry data were collected using a DSC 2920 Modulated DSC, TA instruments and heating at 10 °C/min. Thermo Gravimetric Analysis data were collected using a Hi-Res TGA 2950 Thermogravimetric Analyzer from TA instruments.

**Synthesis of 2,4,6-Pyridinetricarboxylicacid:**[52] To 15.66 gr. (0.13 mole) of 2,4,6-trimethylpyridine, 250 ml of distilled water was added in 1000 ml round bottom flask. The slurry mixture was stirred at room temperature. 163 gr. (1.035 mole) $KMnO_4$ was slowly added on mixture. The red slurry mixture was stirred for 14 hours at room temperature. Then the mixture

was heated to 45-50 °C for 15 hours under reflux. After 15 hours a red mixture turned into black mixture. Solution was left at room temperature for an hour. After the black precipitate settled in the round bottom flask, solution was filtered. A black precipitate collected on filter paper and a clear filtrate observed. Black precipitate was discarded. Clear solution was concentrated to 125 ml solution. Concentrated HCl was added to the solution until the PH was 2.00 .A white precipitate formed after adding HCl, as shown Figure 42. White precipitate was filtered and washed with water. Precipitate was left under hood for a day in order to get rid of excess water in it. Precipitate was dried by vacuum pump. Product identified by H-NMR, C-NMR and Melting Point. Yield was 51%.

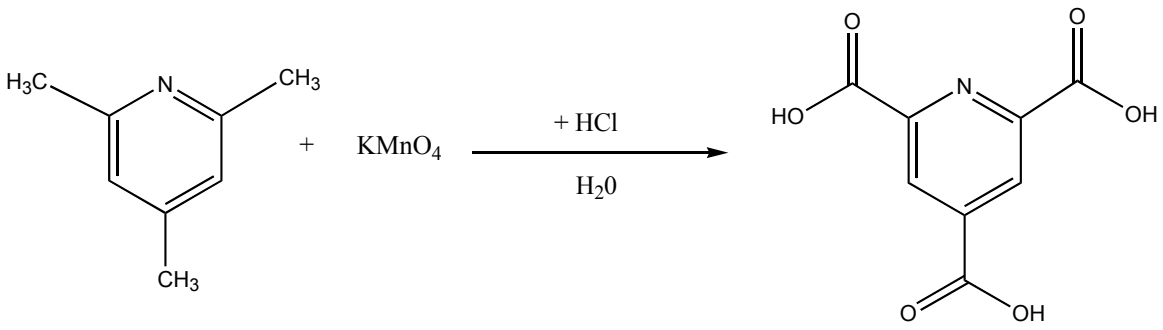


**Figure 42:** Schematic representation of synthesis of 2,4,6-pyridinetricarboxylic acid by oxidation of 2,4,6-trimethylpyridine

**General Method to Synthesize and Crystallize Bis(imidazolium 2,4,6-pyridinetricarboxylate)metal(II) Complexes(1-4).** The following general procedure was used to synthesize and grow crystals of Bis(imidazolium 2,4,6-pyridinetricarboxylate)metal(II) complexes with Co, Ni, Cu, and Zn. 2,4,6 pyridinetricarboxylic acid (e.g., 50 mg, 0.237 mmol) and imidazole (16 mg, 0.237 mmol) dissolved in 5 ml of $H_2O$ and DMSO mixture (9:1, $H_2O$:DMSO) with stirring at approximately 50 °C for 20 min. The appropriate metal chloride or bromide salt (e.g., 0.118mmol) dissolved in the same solvent system in a different beaker with stirring at 40 °C until all solids are disappeared and the solution turned clear. The solution was cooled to room temperature. Metal chloride or bromide solution layered on the 2,4,6-pyridinetricarboxylic acid and imidazole solution carefully by Pasteur pipette. The solution left uncovered. Single crystals of Bis(imidazolium 2,4,6-pyridinetricarboxylate)metal(II) dihydrate formed as clear, colored prisms in solution after several days. Single crystals were removed from solution and dried on filter paper.

It should be noted that formation of metal complexes and subsequent growth of single crystals was achieved by mixing 2,4,6-pyridinetricarboxylic acid, imidazole and metal in 9:1 $H_2O$:DMSO solvent system in a 2:2:1 molar ratio, respectively. This protocol was established

on the basis of experiments involving synthesis and crystallization of the complexes by slow evaporation from the solutions of DMSO in which the relative concentrations of three components were varied systematically. Starting from a 1:1:1 relative ratio of 2,4,6-pyridinetricarboxylic acid, imidazole and metal, the concentration of the individual components was increased incrementally up to a 20-fold excess relative to the other two components. The concentration of pairs of components was also increased incrementally keeping the relative concentration of pairs equal. Large, single crystals of the metal complexes formed when the relative ratio of 2,4,6-pyridinetricarboxylic acid to imidazole was equal. The optimal relative ratio of 2,4,6-pyridinetricarboxylic acid, imidazole and metal was determined empirically to be 2:2:1, respectively.

**Growth of Mixed Crystals.** The following general procedure was used to synthesize and grow mixed crystals that contained complexes between 2,4,6-pyridinetricarboxylic acid, imidazole, and mixtures of two or three different transition metals. Typical experiments were setup as follows. 2,4,6-pyridinetricarboxylic acid (e.g. 50 mg, 0.237 mmol) and imidazole(16 mg, 0.237 mmol) were dissolved in 5 ml of $H_2O$ and DMSO mixture (9:1, $H_2O$:DMSO) with stirring at approximately 50 $^oC$ for 20 min. A pair of metal(II) salts was dissolved in same solvent system in another beaker with stirring at 40 $^oC$ such that the total combined concentration of both metals was one half that of 2,4,6-

pyridinetricarboxylic acid and imidazole(e.g. 0.118 mmol). Metal salt solutions were layered on 2,4,6-pyridinetricarboxylic acid and imidazole solution carefully by using Pasteur pipet. The solution was cooled to room temperature and left uncovered.

Series of mixed crystals that contained $M_1$ and $M_2$ or $M_1$, $M_2$ and $M_3$ were grown from solution by using the procedure mentioned above with different $Co^{2+}$, $Cu^{2+}$, $Zn^{2+}$, $Ni^{2+}$. The compositions of the solutions are in 50 mol % in $M_1$ and 50 mol % in $M_2$ or 33.3 mol % in $M_1$ 33.3 mol in $M_2$ and 33.3 mol% in $M_3$. Incorporation of complexes that contained both metals was evident in each case by the color of the mixed crystal. For example the crystals that contained the red Co complex and the green Ni complex were dark green in color.

**Growth of Composite Crystals.** Composite crystals that contained either Zn and Cu or Co and Ni or Zn and Ni or Ni and Cu were grown using the same procedure to used to form crystal of pure **1-4** described previously. The following procedure describes how composite crystals composed of $M_1$ and $M_2$ were grown. A solution was set up to grow pure crystals of $M_1$. A separate solution was set up to grow crystals of $M_2$. A seed crystal of $M_1$ removed from solution carefully with a spatula and placed immediately into the solution in which crystals of $M_2$ were already starting to form. Uninterrupted epitaxial growth of $M_2$ on the surface of the seed crystal of $M_1$ occurred using this method. When seed crystal of $M_1$ placed

into a solution of $M_2$ in which crystals of $M_2$ had not yet begun to grow. The seed crystal of $M_1$ either dissolved completely or dissolved partially followed by epitaxial growth of $M_2$, depending on how close the solution of $M_2$ was to saturation.

**Determination of X-ray Crystal Structures.** Single-crystal X-ray diffraction data were collected on a Siemens SMART/CCD diffractometer with graphite monochromated Mo K$\alpha$ radiation and equipped with an LT-II low-temperature device. Diffracted data were corrected for absorption using the SADABS program. SHELXS-86 and SHELXL-93 software were used to solve and refine structures on an SGI O2 UNIX platform. Refinement was based on $F^2$. All non-hydrogen atoms were refined anisotropically. Hydrogen atoms on heteroatoms were located and refined with isotropic thermal parameters. The remaining hydrogen atoms were fixed in calculated positions and refined isotropically with thermal parameters based upon the corresponding attached carbon atoms [$U$(H) = 1.2$U_{eq}$($C$)].

**Thermal Behavior of 1-4.** Upon heating in a Meltemp melting point instrument, crystals of **1-4** did not change in shape but turned opaque between 75 and 85 °C, followed by decomposition between 235 and 320 °C. Differential scanning calorimetry showed either four or five endothermic peaks for **1-4**. The last of these peaks corresponds to the

decomposition of crystals observed above. The first peak or two peaks most likely correspond to loss of water from lattice.

**Bis(imidazolium 2,4,6-pyridinetricarboxylate)cobalt(II) Trihydrate 1).** Crystals: dark red prisms. IR ($cm^{-1}$): 3555, 3358, 3111, 2952, 2835, 2566, 1712, 1659; DSC (10 °C/min, T-onset, °C): 109.2, 137.3, 178.0, 227.9, 279.6; TGA (weight loss %): 2% weight loss between 50 °C and 150 °C, 15.5% weight loss between 150 °C and 345 °C.

**Bis(imidazolium 2,4,6-pyridinetricarboxylate)nickel(II) Trihydrate (2).** Crystals: clear green prisms. IR ($cm^{-1}$): 3646, 3375, 3139, 2954, 2641, 1712, 1658; DSC (10 °C/min, T-onset, °C ): 109.2, 156.9, 234.5, 289.6 ; TGA (weight loss %): 1.8% weight loss between 50 °C and 150 °C, 12.6% weight loss between 150 °C and 345 °C.

**Bis(imidazolium 2,4,6-pyridinetricarboxylate)copper(II) Trihydrate (3).** Crystals: clear blue prisms. IR ($cm^{-1}$): 3519, 3108, 2967, 2825, 2562, 1722, 1640; DSC (10 °C/min, T-onset, °C ): 111.2, 120.3, 143.7, 220.1, 270.3, 288.5, 295.0; TGA (weight loss %): 1.7% weight loss between 50 °C and 150 °C, 14% weight loss between 150 °C and 345 °C.

**Bis(imidazolium 2,4,6-pyridinetricarboxylate)zinc(II) Trihydrate (4).** Crystals: colorless prisms. IR ($cm^{-1}$): 3571, 3111, 2964, 2825, 2647, 1721,

1659, 1640; DSC (10 °C/min, T-onset, °C): 125.3, 220.6, 260.7, 265.8; TGA (weight loss %): 2.7% weight loss between 50 °C and 150 °C, 21% weight loss between 150 °C and 345 °C

**References:**


(1) Desiraju, G. R. *Crystal Engineering: The Design of Organic Solids*; Elsevier: New York, 1989; Vol. 54.

(2) Zaworotko, M. J. *Chem. Soc. Rev.* **1994**, 283-288.

(3) Batten, S. R. *J.Angew.Chem., Int.Ad.* **1998**, *37*, 1461-1494.

(4) Hagrman, P. J. *J. Angew. Chem. Int. Ed.* **1999**, *38*, 2638-2684.

(5) Eddaoudi, M. *J. Am. Chem. Soc.* **2000**, *122*, 1391-1397.

(6) Kepert, C. J. *Chem. Commun.* **1998**, 31-32.

(7) Kepert, C. J. *J. Am. Chem. Soc.* **2000**, *122*, 5158-5168.

(8) Kondo, M. *Chem. Mater.* **2000**, *12*, 1288-1299.

(9) Seo, J. S. *Nature* **2000**, *404*, 982-986.

(10) Palmore, G. T. R.; MacDonald, J. C. In *The Amide Linkage: Structural Significance in Chemistry, Biochemistry and Materials Science*; Greenberg, A., Breneman, C. M., Liebman, J. F., Eds.; John Wiley and Sons: New York, 2000, pp 291-336.

(11) Vögtle, F. *Supramolecular Chemistry: An Introduction*; John Wiley and Sons: New York, 1991.

(12) Yaghi, O. M.; Li, G.; Li, H. *Nature* **1995**, *378*, 6558.

(13) Yaghi, O. M.; Li, G. *Angew. Chem. Int. Ed. Engl.* **1995**, *34*, 307.

(14) Aakeröy, C. B.; Seddon, K. R. *Chem. Soc. Rev.* **1993**, 397-407.

(15) Anthony, A.; Desiraju, G. R.; Jetti, R. K. R.; Kuduva, S. S.; Madhavi, N. N. L.; Nangia, A.; Thaimattam, R.; Thalladi, V. R. *Cryst. Eng.* **1998**, *1*, 1-18.

(16) Yaghi, O. *Acc. Chem. Res.* **1998**, *31*, 474-484.

(17) Duchamp, D. J. *Acta Crystallogr. Sect. B* **1969**, *25*, 5-19.

(18) Ermer, O. *J. Am. Chem. soc.* **1988**, *110*, 3747-3754.

(19) Chin, D. N.; Zerkowski, J. A.; MacDonald, J. C.; Whitesides, G. M. In *Organised Molecular Assemblies in the Solid State*; Whitesell, J. K., Ed.; John Wiley and Sons: New York, 1999, pp 185-253.

(20) Etter, M. C. *J. Phys. Chem.* **1991**, *95*, 4601-4610.

(21) MacDonald, J. C.; Whitesides, G. M. *Chem. Rev.* **1994**, *94*, 2383-2420.

(22) Leiserowitz, L. *J. Chem. Soc. A.* **1969**, 2372.

(23) Leiserowitz, L. *Acta Crystallogr.* **1978**, *B34*, 1230.

(24) Wuest, J. D. *J. Am. Chem. Soc.* **1991**, *113*, 4696-4968.

(25) MacDonald, J. C. *J. Am. Chem. Soc.* **2000**, *122*, 11692-11702.

(26) Bernstein, J.; Etter, M. C.; MacDonald, J. C. *J. Chem. Soc., Perkin Trans. 2* **1990**, 695-698.

(27) Bernstein, J. *J. Phys. D: Appl. Phys.* **1993**, *26*, B66-B76.

(28) Zerkowski, J. A.; MacDonald, J. C.; Whitesides, G. M. *Chem. Mater.* **1997**, *9*, 1933-1941.

(29) Chin, D. N.; Palmore, G. T. R.; Whitesides, G. M. *J. Am. Chem. Soc.* **1999**, *121*, 2115-2122.

(30) Matzger, A. J. *Crystal Growth & Design* **2002**, *2*, 501-503.

(31) Atencio, R.; Biradha, K.; Zaworotko, M. J. *Cryst. Eng.* **1998**, *1*, 203.

(32) Christie, S. D.; Subramanian, S.; Zaworotko, M. J. *J. Chem. Soc., Chem. Commun.* **1994**, 2563.

(33) Li, H.; Davis, C. E.; Yaghi, O. M. *J. Am. Chem. Soc.* **1998**, *120*, 2186.

(34) Munakata, M.; Wu, L. P.; Kuroda-Sowa, T. *Bull. Chem. Soc. Jpn.* **1997**, *70*, 1727-1743.

(35) Sharma, C. V. K.; Rogers, R. D. *Cryst. Eng.* **1998**, *1*, 19-38.

(36) Yaghi, O. M.; Davis, C. E.; Li, H. *J. Am. Chem. Soc.* **1997**, *119*, 2861.

(37) Yaghi, O. M.; Li, H.; Groy, T. L. *Inorg. Chem.* **1997**, *36*.

(38) Yaghi, O. M.; Reinke, T. M.; Eddaoudi, M. *J. Am. Chem. Soc.* **1999**, *121*, 1651.

(39) Yaghi, O. M.; Li, H.; Groy, T. L. *J. Am. Chem. Soc.* **1996**, *118*, 9096.

(40) Yaghi, O. *Science* **2002**, *295*, 469-472.

(41) Aakeröy, C. B.; Beatty, A. M. *Cryst. Eng.* **1998**, *1*, 39-49.

(42) Bailey, R. D.; Hook, L. L.; Powers, A. K.; Hanks, T. W.; Pennington, W. T. *Cryst. Eng.* **1998**, *1*, 51-66.

(43) Bhyrappa, P.; Wilson, S. R.; Suslick, K. S. *J. Am. Chem. Soc.* **1997**, *119*, 8492-8502.

(44) Falvello, L. R.; Pascual, I.; Tomas, M. *Inorg. Chem. Acta* **1995**, *229*, 135-142.

(45) Falvello, L. R.; Pascual, I.; Tomas, M.; Urriolabeitia, E. P. *J. Am. Chem. Soc.* **1997**, *119*, 11894-11902.

(46) Schauer, C. L.; Matwey, E.; Fowler, F. W.; Lauher, J. W. *J. Am. Chem. Soc.* **1997**, *119*, 10245-10246.

(47) MacDonald, J. C.; Dorrestein, P. C.; Pilley, M. M. *Crystal Growth & Design* **2000**, *submitted*.

(48) Aakeröy, C. B.; Hitchcock, P. B.; Seddon, K. R. *J. Chem. Soc., Chem. Commun.* **1992**, 553-555.

(49) Aakeröy, C. B.; Hitchcock, P. B. *Acta Cryst.* **1994**, *C50*, 759-761.

(50) Aakeröy, C. B.; Nieuwenhuyzen, M. *J. Am. Chem. Soc.* **1994**, *116*, 10983-10991.

(51) Gandour, R. D.; Nabulsi, N. A. R.; Fronczek, F. R. *Journal of the American Chemical Society* **1990**, *112*, 7816-7817.

(52) Mkochowski, J. *Tetrahedron* **1979**, *36*, 123-129.